Spider's Orb Web: Implications of Structural Hierarchies to Materials-based Evolution

by

Anna Tarakanova

B.S. Applied and Engineering Physics
Cornell University, 2011

Submitted to the Department of Civil and Environmental Engineering in partial fulfillment of the requirements for the degree of
Master of Science in Civil and Environmental Engineering
at the
Massachusetts Institute of Technology
September 2015

Signature of Author: Signature redacted
Department of Civil and Environmental Engineering
August, 20 2015

Certified by: Signature redacted
Markus J. Buehler
Professor of Civil and Environmental Engineering
Thesis Supervisor

Accepted by: Signature redacted
Heidi Nepf
Donald and Martha Harleman Professor of Civil and Environmental Engineering
Chair, Graduate Program Committee

Table of Contents

Spider's Orb Web: Implications of Structural Hierarchies to Materials-based Evolution

by

Anna Tarakanova

Submitted to the Department of Civil and Environmental Engineering on August 20, 2015 in partial fulfillment of the requirements for the degree of
Master of Science in Civil and Environmental Engineering

Abstract

Among a myriad of spider web geometries, the orb web presents a fascinating, exquisite example in architecture and evolution. Its structural component, the silk protein, is an exemplary natural material because its superior properties stem intrinsically from the synergistic cooperativity of hierarchically-organized components, rather than from the particular properties of the building blocks themselves. By bridging together different levels of hierarchy in the web, we elucidate the mechanisms by which structure at each composite level contributes to organization and material phenomena at subsequent levels, demonstrating that the web is a highly adapted system where both material and hierarchical structure across all length-scales is critical for its functional properties. Further, the material hierarchy scheme within the orb web is exploited to address questions of silk evolution. Spider orb webs can be divided into two categories distinguished by the capture silk used in construction: cribellate orb webs composed of pseudoflagelliform silk coated with dry cribellate threads and ecribellate orb webs, composed of viscid flagelliform silk fibers, coated by adhesive glue droplets. Cribellate capture silk is generally stronger but less extensible than viscid capture silk and a body of phylogenic evidence suggests that cribellate capture silk is more closely related to the ancestral form of capture spiral silk. Here, we use a coarse-grained web model to investigate how the mechanical properties of spiral capture silk affect the behavior of the web system, illustrating that more extensible capture spiral silk yields a decrease in the web's energy absorption, suggesting that the function of the capture spiral shifted from prey capture to other structural roles. Additionally, we observe that in webs with

more extensible capture silk, the effect of thread strength on web performance is reduced, indicating that thread extensibility is a dominant driving factor in web diversification. In this thesis, we propose a novel model-centered materials-hierarchy based approach to studying evolutionary trends and suggest possible applications for other fields.

Thesis Supervisor: Markus J. Buehler
Title: Professor of Civil and Environmental Engineering

List of Publications

A. Tarakanova, M.J. Buehler, "A materiomics approach to spider silk," *JOM*, Vol. 64(2), 214-225, 2012.

Tarakanova, M.J. Buehler, "The role of capture spiral silk properties in the diversification of orb webs," *Journal of the Royal Society Interface*, Vol. 9(77), pp. 3240-3248, 2012.

S.W. Cranford, A. Tarakanova, N. Pugno, M.J. Buehler, "Nonlinear material behaviour of spider silk yields robust webs," *Nature*, Vol. 482, pp. 72-76, 2012 (cover article)

Background and Motivation

Spider Silk: A structural mammoth of tiny proportions

For decades, spider silk has captivated the attention of researchers for its outstanding mechanical properties. Silk is a model prototype of Nature's design, combining exceptional mechanical qualities that surpass high energy-absorbing materials such as Kevlar and carbon fiber, with an extremely light-weight alternative (Agnarsson, Kunter, & Blackledge, 2010; J.M. Gosline, P.A. Guerette, C.S. Ortlepp, & K.N. Savage, 1999; B. O. Swanson, Anderson, Digiovine, Ross, & Dorsey, 2009; F. Vollrath, 2010). A combination of high tensile strength on par with steel (at 1-2 GPa (B. O. Swanson et al., 2009)) and extensibility (up to 60% maximum strain (B. O. Swanson et al., 2009)) results in superior toughness and exceeding performance when normalized by its density.

Silk fibroin originates in specialized abdominal glands (J. M. Gosline, P. A. Guerette, C. S. Ortlepp, & K. N. Savage, 1999). All known spider species produce some kind of silk, which is extracted through spinnerets in the process of deposition (P. A. Guerette, D. G. Ginzinger, B. H. F. Weber, & J. M. Gosline, 1996). A single spider has the ability to produce silks with mechanically distinct properties that correspond to a unique silk gland and correlate with a specific function (Denny, 1976). Considering the diversity of

existing silk types, spider silk is an example of a biological protein fiber where the hierarchical structure—exhibiting weak hydrogen bonding at its core—regulates material behavior on multiple length scales.

Natural Hierarchies in the Spider's Web

The diversife functionality of protein-based materials is often a result of hierarchical structure, rooted in the molecular composition, which expands the material design space to incorporate multiple levels (Buehler, 2010; Buehler & Yung, 2009; Sen & Buehler, 2011). The underlying composition of such systems may be founded on weak building blocks, which are abundantly available, accessible to low-energy processing, or have an innate capacity to self-assemble. Characterization of material systems on multiple length scales emerges by bridging weak building block components to particular mechanical behaviors at the macroscale. It is these layers of hierarchy that determine the specific characteristics of materials at the macroscale and drive their function and evolution.

Spider orb webs serve as a prime example of a highly ordered, complex system defined and governed by underlying lower length scale building blocks. Specifically, silk protein, the composing material of webs, drives function and plays a role in the evolution of webs. The hierarchies in silk's material composition are illustrated in

Figure 1.1. Silk's lowest level of hierarchy is based on its primary protein structure, defined by a sequence of amino acids, which is responsible for subsequent folding mechanisms that lead to the defining molecular structure. Residue segments form secondary structures, including crystalline beta sheets, 3_1 helices and beta turns (Heim, Romer, & Scheibel, 2010b). The chemical bonding within these structures determines their material properties: dense hydrogen bonds make up the stiffer crystals, while dispersed hydrogen bonds join together extendable helices and beta turns. Joined arrangements of the secondary structures create a network of beta sheet crystals embedded in an amorphous meshwork of less orderly structures.

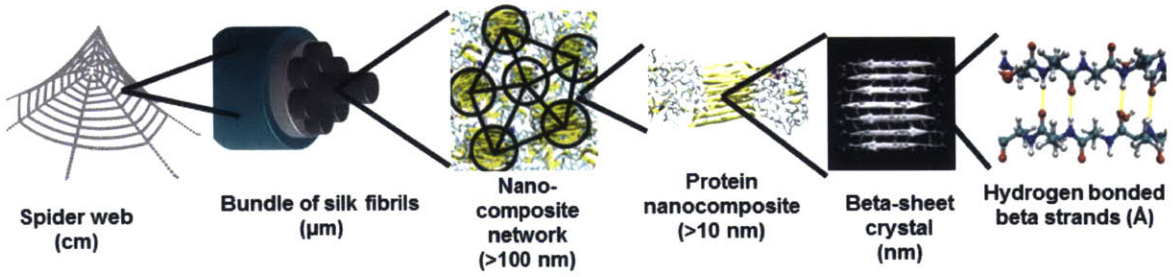

Figure 1.1 | Hierarchical structure of spider silk. Multiple hydrogen-bonded beta strands make up a beta-sheet nanocrystal; a bundle of nanocrystals compose a crystalline domain embedded in semi-amorphous domains consisting of more disordered subunits; together these form the protein nanocomposite structure; protein chains are combined in a larger-scale network that forms fibrils with diameters of less than 100 nm; bundles of fibrils form the fibers with diameters of several micrometers, making up the threads found in a spider web. Figure modified from (Tarakanova & Buehler, 2012).

Protein chains combine into silk fibrils that bundle together into fibers, forming threads in the web. Silk's unique material properties are exploited by spiders to construct

geometrically organized web structures to serve a variety of functions, from effective prey capture to nest construction (F. Vollrath, 1999).

The spider's orb web is a useful model system to elucidate material function as the interplay of the material's building blocks and gain a fundamental understanding of structure-function relationships across different length scales (Spivak, Giesa, Wood, & Buehler, 2011). A series of models to analyze the connection between composition and mechanical behavior across length scales is outlined in **Table 1.1**. A notable result from these studies is that the observed properties of silk derive not from the superior material behavior at each level of hierarchy but rather from the combined or complementary function of building blocks at each length scale.

Structure	**Hierarchical Level**	**Description**	**Key mechanism & Experimental Validation**
Amino acid sequence	Primary protein structure (Å)	The primary protein structure is composed of a sequence of amino acid residues which define the folding of subsequent hierarchical levels. In silk, poly-alanine regions are responsible for stiff cross-linking domains while glycine-rich regions are found in structures within amorphous domains.	Basic building block that dictates secondary protein structure. Experimental techniques such as NMR and x-ray diffraction are limited in their atomic resolution for complex materials, so molecular dynamics permits a discrete qualification of primary structure through folding mechanisms. Recent work has been successful in sequencing silk genes and using this information to generate recombinant engineered versions of the natural protein

			(Ayoub, Garb, Tinghitella, Collin, & Hayashi, 2007). Changes of amino acid sequence can be experimentally realized through genetic engineering or peptide synthesis.(Rising, Widhe, Johansson, & Hedhammar, 2010)
Beta-sheet nanocrystals	Secondary protein structure (nm)	The secondary protein structure defines local conformations, such as alpha helices and beta turns. Beta sheets crystals in silk have a critical size of 2 to 4 nm, exhibiting exceptional strength due to cooperative hydrogen bonding between beta strands. This invokes a highly dissipative stick-slip mechanism that provides the basis for larger-scale toughness and strength.	Nanoconfinement of crystal optimizes cooperative hydrogen bond activity, resulting in shear deformation shown to result in most regulated and least catastrophic failure, through the self-healing capacity of hydrogen bonds. Critical crystal sizes can be validated against experiment, based on AFM images(Du et al., 2006) and diffraction techniques (Du et al., 2006).
Protein composite (beta-sheet crystals, beta turns, 3_1 helices)	Tertiary protein structure (~ 10-20 nm)	Tertiary protein structure is the three-dimensional arrangement of interacting secondary structures. The interplay between beta sheet crystals and amorphous domains ensures strength and extensibility of the composite structure.	The cooperative interplay and load-balance of protein composite domains achieves a unique hyperelastic material behavior in silk. Molecular dynamics can identify nanoscale protein-unfolding regimes, difficult to discern experimentally.
Fibrils	(~100 nm)	Fibrils exhibit dimensions of 50±30 nm in diameter, where cohesive interaction of protein domains composing the fibril is responsible for homogeneous load distribution upon loading, for optimal strength.	Nanoconfinement of fibril size results in homogeneous deformation of all protein domains within the fibril, thereby achieving greatest strength and toughness through contributions of many protein components acting together. Optimal fibril size is validated e.g. through SEM images (Du et al., 2006).
Fibers	(~1-2 μm)	Bundles of fibrils into fibers	Bundling of several

		enhance mechanical properties of silk threads.	geometrically confined fibrils into a fiber enhances material properties by reaching homogeneous deformation state (flaw tolerance). Structure and geometry of fibers can be visible via SEM imaging (Du et al., 2006).
Spider web	(>cm)	Spider web geometry and material composition determine the deformation mechanisms of the web, responsible for function.	Localization of failure due to yielding-stiffening behavior during deformation. *In-situ* experiments conducted on garden webs show a similar result (S.W. Cranford 2011). Geometry in the model is obtained from a natural orb-web (S.W. Cranford 2011; Brook O. Swanson, Blackledge, & Hayashi, 2007).

Table 1.1. Summary of the structural hierarchy of spider web and key mechanisms that define mechanical function, spanning length scales from angstroms to centimeters. Table modified from (Tarakanova & Buehler, 2012).

Silk hierarchy can be characterized through a bottom-up modeling approach whereby lower length-scale parameters (the building blocks of the system for a subsequent hierarchical level) are linked to coarser, larger length-scales. Mechanical characterization and an understanding of deformation mechanisms serves as a link to higher order hierarchies, contributing to a powerful feedback loop where the bottom-up modeling approach catalyzes insights we gain at each layer of the material ladder (**Figure 1.2**).

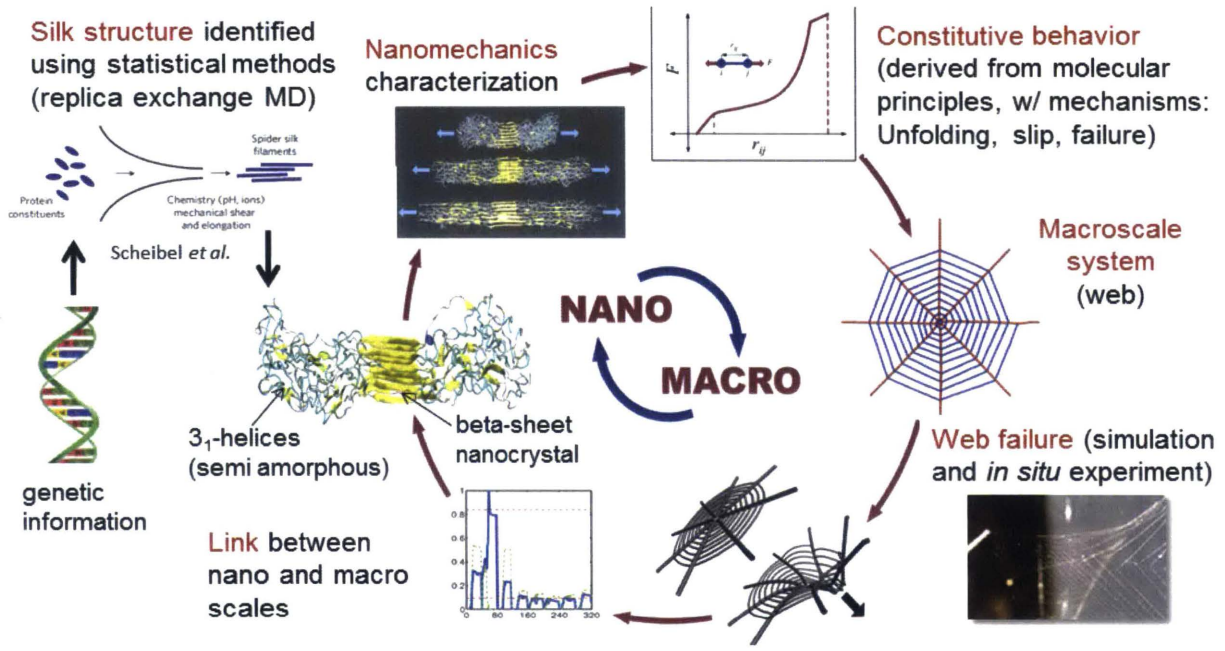

Figure 1.2 | Multiscale approach to the study of a spider's web. Summary of the multiscale approach for spider web analysis, linking the molecular scale to the macroscale. Replica Exchange Molecular Dynamics is used to identify protein structure based on genetic makeup; mechanical testing characterizes a constitutive behavior; molecularly-derived behavior is incorporated into a macroscale web system; web scale deformation experiments link macroscale deformation to molecular mechanisms (Rising et al., 2010). Figure modified from (Tarakanova & Buehler, 2012).

We conceive that the ability to analytically describe multiple levels of hierarchical behavior from the building blocks opens the opportunities for creating tunable materials and offers the possibility of controlling properties at multiple scales simultaneously. Such analysis projects the possibility of new design paradigms in areas of application ranging from high performance fibers and multifunctional materials produced from artificially spun silk or derived materials (Omenetto & Kaplan, 2010; Rammensee, Slotta, Scheibel, & Bausch, 2008), to novel material platforms for tissue

engineering or structural applications in the defense and aerospace industries (Buehler & Yung, 2009; Vepari & Kaplan, 2007).

Silk Through Time: Factors in the Evolutionary History of Spider Silk

Beyond spider silks' remarkable properties of great strength and extensibility, well-documented by the silk community, the large number and diversity of silks found in Nature have inspired significant research (Agnarsson et al., 2010; Denny, 1976; Heim et al., 2010b; Omenetto & Kaplan, 2010; Tarakanova & Buehler, 2012; Vepari & Kaplan, 2007; F. Vollrath, 1999). The success of the spider is evident from the great diversity of spider species, numbering over 39,000 to date (J. A. Coddington, Giribet, Harvey, Prendini, & Walter, 2004). The variation in properties and correlated differences in mechanical performance and specific function can be compared across spider phylogeny (Madsen, Shao, & Vollrath, 1999). Broad phylogenic studies show repeatable variation in silk properties across species. Individual and behavioral variation further complicates these interconnections across species within spider evolution (B. O. Swanson et al., 2009).

The phylogenic comparisons across spider species can be navigated through a systematic comparison of silk sequences. The first silk sequences (of spider dragline silk) were identified in 1990 (Xu & Lewis, 1990). These sequences contained highly ordered, repetitive polyalanine domains interspersed with glycine-alanine and glycine-proline-glycine repeats. Later molecular modeling studies identified the nanocomposite structure within silk protein fibers, where beta sheet crystal regions were embedded in amorphous regions, contributing to strength and elasticity of the protein, respectively (Sinan Keten & Markus J. Buehler, 2010; S. Keten & M.J. Buehler, 2010; Keten, Xu, Ihle, & Buehler, 2010). Subsequently, other types of silks were sequenced, including dragline, capture spiral, egg-casing and prey-wrapping silks for a number of different species (Garb & Hayashi, 2005; P. A. Guerette, D. G. Ginzinger, B. H. Weber, & J. M. Gosline, 1996; Hayashi, Blackledge, & Lewis, 2004; Hayashi & Lewis, 2000; Tian & Lewis, 2005). These sequences vary in the composition, length and number of repeated motifs across different silk types within a species and across different species (B. O. Swanson et al., 2009). The mechanical differences stem, at least in part, from an evolution of the composing parts, which in turn plays into the mechanisms and functions of the individual spiders and spider silks.

External factors may also contribute to changes in silk morphology and material properties. Such adaptive changes come in response to shifted spinning patterns and

orientations or an alteration in the available food sources (Boutry & Blackledge, 2008; Perez-Rigueiro et al., 2010; Tso, Wu, & Hwang, 2005; F. Vollrath, Madsen, & Shao, 2001). There is evidence that spiders can actively change the amino acid composition of their silk, by adjusting modes of silk extraction through spinning rate and sheer stress at point of silk production (C. L. Craig et al., 2000; Perea et al., 2013).

Across different types of silk, one of the most variable is the capture spiral silk of orb webs. This stretchy, rubber-like silk is only produced by spiders in the Orbicularian clade of araneomorph spiders and functions in the capture and retention of flying insects in the orb web (Opell & Bond, 2001). Interestingly, the material properties of the silks seem to be evolutionary correlated, exhibiting a tradeoff between strength and extensibility (Brook O. Swanson et al., 2007). In the remainder of this thesis, we focus on the evolutionary implications of this trend, from a mechanical, structure-hierarchy-function paradigm, by integrating material behavior of different silks into the functional interplay within an orb web model.

Evolutionary Trends in the Capture Silk of Orb Webs

From the plethora of spider species, orb-weavers have not surprisingly captured significant attention, as a result of the near-perfect, beautiful architecture of the orb in combination with superior material properties of its silk (Krink & Vollrath, 1997).

Orb-weaving spiders that can be found today belong to the Orbicularian clade (Blackledge et al., 2009). This clade is divided into two spider superfamilies, the Araneoidea and Deinopoidea (Griswold, Coddington, Hormiga, & Scharff, 1998). The first orb-webs appeared more than 200 million years ago and by 145 million years ago the major orb-weaving families were already present (Harmer, Blackledge, Madin, & Herberstein, 2011; Penney & Ortuno, 2006; Selden, 1989; Zschokke, 2003). The appearance of orb-webs in the Triassic period correlated with the production of strong major ampullate silk, which makes up the radially extending threads in a typical orb-web (C. Craig & Brunetta, 2010). Along with major ampullate silk, cribellate silk first appeared at this time, composing the capture spiral of the ancient common ancestor of modern orb-web weaving spiders and found today in the Deinopoidea superfamily (C. Craig & Brunetta, 2010). Deinopoids use dry fuzzy cribellate silk in their capture spiral threads to build horizontally oriented webs and prey on slow, walking organisms by trapping them with sticky cribellate microfibrils, covering the anchoring thread fibers

(W. Eberhard & Pereira, 1993; Opell, 1994). By the time orb-webs were abundant, in the early Cretaceous period, flagelliform silk, currently found in the capture threads of the Araneoidea superfamily, appeared on the evolutionary spectrum. Araneoids, by contrast, construct vertically oriented webs, building their capture spirals out of the stretchy flagelliform silk covered with sticky aqueous glue droplets for catching quick flying prey (Peters, 1995; Tillinghast, Townley, Wight, Uhlenbruck, & Janssen, 1993; F. Vollrath et al., 1990; F. Vollrath & Tillinghast, 1991). By comparing spinning behavior, spinneret and leg anatomy and other anatomical features of the two superfamilies, in addition to finding a flagelliform silk gene but not flagelliform silk thread in deinopoids, arachnologists became convinced that the orb-web evolved a single time (J. Coddington, 1982; J. A. Coddington & Levi, 1991) and that cribellar silk was older, and more primitive (Blackledge & Hayashi, 2006; Garb, DiMauro, Vo, & Hayashi, 2006). Araneoids, on the other hand, are much more diverse, occupying a larger range of niches and can therefore be qualified as being evolutionarily "superior" to their sister deinopoid counterparts.

Various studies have been conducted to address the question of divergence between the two superfamilies, in particular to understand the evolutionary advantage of the Araneoidea. Opell hypothesized that the economical sticky capture silk produced by araneoids maximizes stickiness per capture area, yielding an evolutionary advantage on

the basis of efficiency and economy (Opell, 1998, 1999). In studies comparing trends in spider weight, orb-web architecture and capture area, Opell concluded that araneoids were better equipped to dissipate kinetic energy of faster, larger prey (Opell, 1997). Blackledge *et al.* (Blackledge et al., 2009) contended that the evolutionary advantage of a simpler spinning process of the araneoids allowed them to achieve such diversity. To produce cribellar threads, a spider spins a core thread which is followed by a long, arduous process of adding a layer of microfibers which gives cribellar silk its properties (Blackledge & Hayashi, 2006). On the other hand, to produce flagelliform silk the spider quickly spins a single layer, covering the thread with aqueous glue as it is spun- thus rendering the process metabolically advantageous. Likewise, Swanson *et al.* (B. O. Swanson et al., 2009) claimed that spinning morphology and variation in silk sequence are the driving evolutionary factors. In addition to a shift in spinning mechanism, Blackledge *et al.* (Blackledge et al., 2009) found a divergence from substrate-bound webs, arguing for behavioral implications to web evolution. Similarly, Vollrath *et al.* (Fritz Vollrath & Selden, 2007) found behavior to be a driving force in spider evolution.

A particularly notable shift through evolutionary time is the switch in capture silk thread material properties, which was recently characterized by the most extensive study to date on silk properties in a range of species (**Figure 1.3**) (Brook O. Swanson et al., 2007). The operational role of capture silk in orb-webs is crucial to prey interception

and capture (C. L. Craig, 1987; Opell, 1996, 1999). It is also the most energetically costly component for spiders to make in both superfamilies (Sherman, 1994).

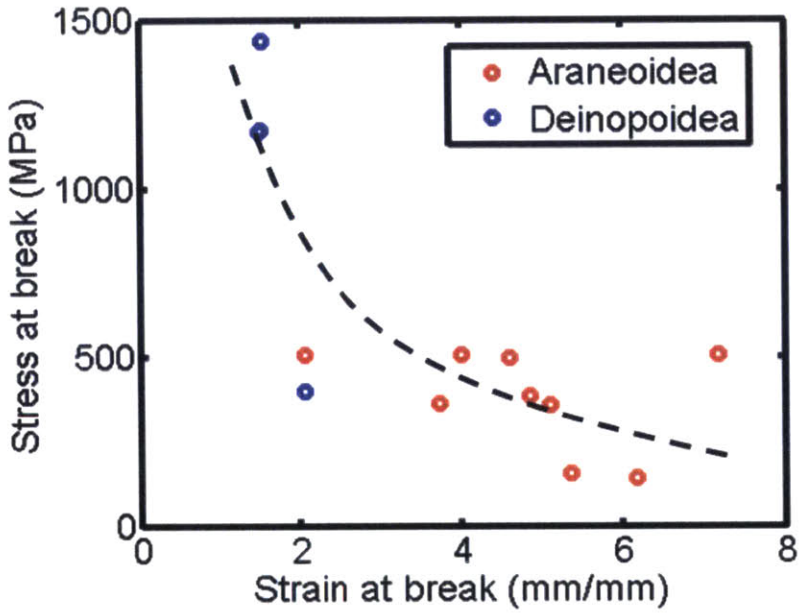

Figure 1.3 | A wide diversity of material properties is exhibited by capture silk threads in orb webs. Stress and strain of spiral capture threads at break were quantified in empirical tensile tests for thirteen spider species, adapted from Swanson *et al.* (Brook O. Swanson et al., 2007). Capture silks in the Deinopoidea super family tend to have higher ultimate stresses and lower ultimate strains than capture silks found in the Araneoidea super family. This material "trade-off" correlates with an apparent evolutionary advantage attributed to the more numerous araneoids. Figure modified from (Tarakanova & Buehler, 2012).

The apparent trade-off in strength and extensibility of silks between the two superfamilies (Opell & Bond, 2001; Brook O. Swanson et al., 2007) indicates that increased extensibility and reduced strength are evolutionary advantageous. It has been suggested that the vertical orientation of araneoid webs results in greater impact forces

by faster, flying prey than those found in deinopoid webs (C. L. Craig, 1987; W. G. Eberhard, 1989; Opell, 1997). This predicts that the energy absorption capacity of webs of the more recently evolved araneoid species is increased, thereby rendering these "newer" webs evolutionary advantageous.

Few studies have explicitly considered the relationship between material variation across the evolutionary spectrum and the connection to energy absorptive capacity of webs. Kohler *et al.* (Kohler & Vollrath, 1995) conducted tensile tests on species of both superfamilies to compare mechanical properties of the threads, proposing a different mechanistic approach of energy dissipation. They observed that energy was dissipated by araneoid webs through absorption by extensibility, while deinopoids dissipated energy by the friction of the small cribellar microfibrils.

Craig (C. L. Craig, 1987) considered web models to study the relationship of web energy absorption to various architectural web features including radial prestress, the number of web radials and spirals, and the angle of the web with respect to web loading. Craig measured energy-absorption capabilities of five real araneoid webs based on artificial loading experiments and through calculations of the kinetic energy of prey caught by each web. However, she did not explicitly consider the silk material property effect on energy absorption. She concluded that web geometry is a key factor for high-energy

absorbing webs while properties of individual threads determined energy dissipation in small low-energy absorbing webs, suggesting furthermore that the evolutionary advantage accompanied the latter, thereby increasing the reliability on individual silk properties in the development of webs.

Lin *et al.* (L. H. Lin, Edmonds, & Vollrath, 1995) considered a finite-element model of a web and found that aerodynamic damping plays a crucial role in energy dissipation during prey capture, however only for one species of spider. Sensenig *et al.* (A. Sensenig, Agnarsson, & Blackledge, 2010) studied 22 species of spiders and focused on the connection between silk quality and web geometry, demonstrating that larger spiders spin higher quality silk with improved material properties and "sparser" web architectures, though no direct connection was drawn between web mechanics and evolutionary implications.

The consequences on web mechanics due to the apparent shift from stronger, less extensible threads in deinopoids to weaker more elastic threads in araneoids has never been explicitly studied, though several authors have proposed that the role of a material transition is key in spider evolution (Blackledge & Hayashi, 2006; Bond & Opell, 1998). In our studies, we test the hypothesis that an observed material behavior shift is responsible for araneoids' proposed ability to absorb and dissipate energy better than

their common ancestor with the more primitive deinopoids (C. Craig & Brunetta, 2010; C. L. Craig, 1987; Harmer et al., 2011; Opell, 1997). We use an inverse approach to evolution: the products of the evolutionary process within a web model facilitate the understanding of mechanistic advantages grounding the process itself. We ask the question: what are the mechanical advantages of particular "chosen" structures, in this case the capture silks of the more diverse araneoid species.

Materials and Methods

Web model geometry, connectivity, and elements

We mimic a realistic orb web structure and approximate the orb web by an arithmetic spiral (F. Vollrath & Mohren, 1985; Zschokke & Vollrath, 1995). The spiral is an Archimedes' spiral, defined by the polar equation:

$$R(\theta) = \alpha \cdot \theta, \qquad (1)$$

The coils of successive turns are spaced in equal distances, dR, where $dR = 2\pi\alpha$. For all models generated, $\alpha = 0.005$ m, resulting in $dR \approx 31$ mm. The spiral is defined by prescribing the angle θ in a range from 360° to 3600°. To ensure that the inter-particle spacing is approximately the prescribed inter-particle distance, the spiral arc length between consecutive particles, ds, is calculated, where:

$$ds = s(\theta_i) - s(\theta_{i-1}), \tag{2}$$

and

$$s(\theta_i) = \frac{1}{2}\alpha\left[\theta_i\sqrt{1+\theta_i{}^2} + \ln\left(\theta_i + \sqrt{1+\theta_i{}^2}\right)\right]. \tag{3}$$

A constant increment in angle, $d\theta$, results in a monotonically increasing ds. Consequently, we implement an iterative loop to reduce $d\theta$ as the spiral radius increases, ensuring that $ds < 1.05r_0$, where r_0 is the initial inter-particle spacing equal to 0.01 m. The numerical factor 1.05 is included to provide stochastic variation in structure, representing a more realistic spider web as opposed to a perfect spiral, and also accounts for the slight difference between arc length and chord length between consecutive particle positions. Radial threads are prescribed at regular intervals ($d\theta = 45°$), and span 0.4 m in the radial direction.

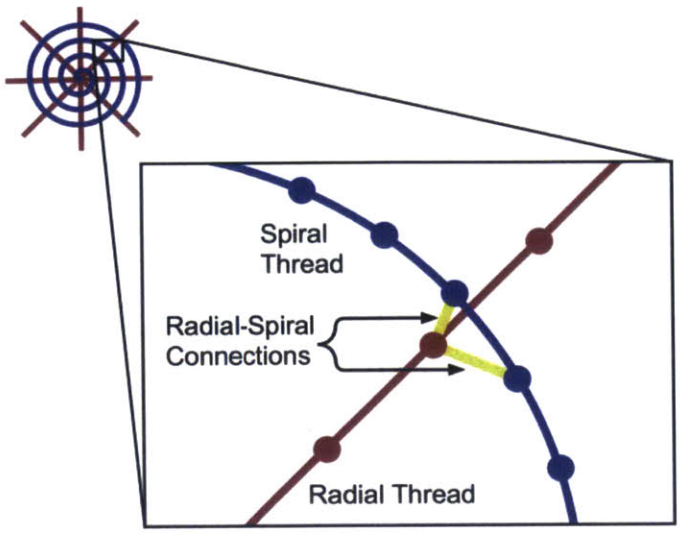

Figure 2.1 | Schematic of radial-spiral connection configuration. The overlaid spiral silk thread is attached to the radial threads by bonds reflective of attachment cement of physical orb webs. The material behaviour of the connections is that of the radial threads. Figure modified from (Cranford, Tarakanova, Pugno, & Buehler, 2012).

In physical webs, the interconnection of the different silks in an orb-web is accomplished via a gluey, silk-like substance termed "attachment cement" originating from the piriform gland of spiders (Gosline, Demont, & Denny, 1986; Heim, Keerl, & Scheibel, 2009; Heim, Romer, & Scheibel, 2010a; Romer & Scheibel, 2008). Here, we account for these discrete or non-continuous radial-spiral connections via the introduction of "attachment bonds" to reflect the attachment cement of physical orb webs (**Figure 2.1**).

There exist four types of bonds and springs (elements) for connectivity in the web models considered:

1. **Radial bonds** (representing radial threads), consisting of 40 particles spaced 10 mm apart in the radial direction, connected consecutively.
2. **Inner radial circle connections**, to avoid stress concentration by a common connection point. Each radial thread is connected to a small, inner circle at the centre of the spiral with a radius of 10 mm consisting of 16 particles. The stress-strain behaviour is that of the radial threads.
3. **Spiral bonds** (representing spiral threads) in a continuous spiral, particles spaced approximately 10 mm apart, connected consecutively.
4. **Radial-spiral connections** (representing silk-like "attachment cement"). Connection bonds linking spiral to radial threads at cross-over regions if the distance between the spiral bead and nearest radial bead is less than 8 mm. There are 1 to 3 connections per cross-over region. Stress-strain behaviour is that of the radial dragline threads.

Material models

We parameterize and implement two types of material behavior: (i) atomistically derived dragline silk behavior of the radial threads in an orb web and (ii) a series of

empirically parameterized capture silk material behaviors found in spiral threads. Theoretical material trends representative of capture silk across different species are examined to elucidate the patterns of spiral thread evolution.

Atomistically derived dragline silk

A combination of linear and exponential functions determines the stress-strain behaviour of the dragline silk of the radial elements in the orb web, defined by four parameters reflecting stiffness, and three critical strains (**Figure 2.2**). This formulation is a result of the interplay of different domains within silk protein, specifically, the combination of β-sheet nanocrystals and amorphous protein domains (Nova, Keten, Pugno, Redaelli, & Buehler, 2010).

The stress-strain function is expressed as:

$$\sigma(\varepsilon) = \begin{cases} E_1\varepsilon & , 0 \le \varepsilon < \varepsilon_y \\ \exp[\alpha(\varepsilon - \varepsilon_y)] + \beta(\varepsilon - \varepsilon_y) + C_1 & , \varepsilon_y \le \varepsilon < \varepsilon_s \\ E_2(\varepsilon - \varepsilon_s) + C_2 & , \varepsilon_s \le \varepsilon < \varepsilon_b \\ 0 & , \quad \varepsilon \ge \varepsilon_b \end{cases}. \tag{4}$$

It is defined by four parameters (E_1, E_2, α, and β) reflecting stiffnesses, and three corresponding critical strains (ε_y, ε_s, ε_b) (**Table 2.1**).

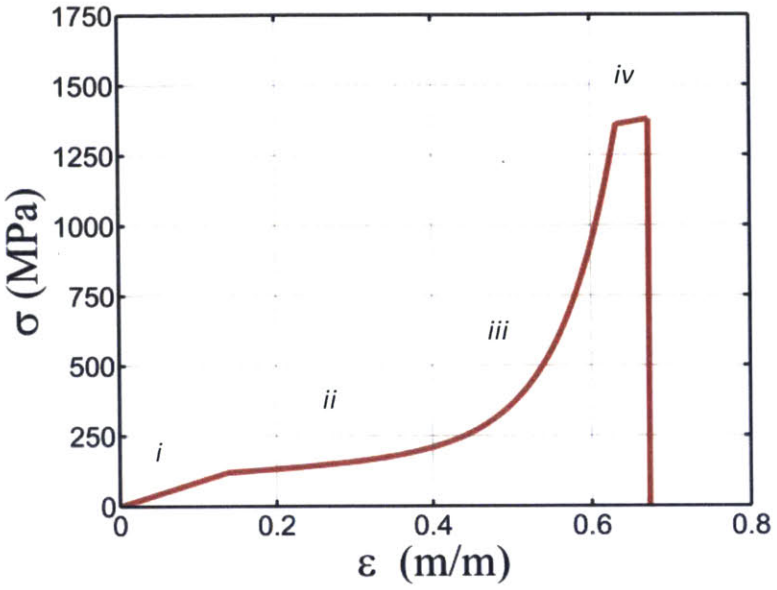

Figure 2.2 | Stress-strain behaviour implemented for atomistically derived dragline silk. The nonlinear behaviour is separated into four regimes: (*i*) linear until yielding; (*ii*) entropic unfolding; (*iii*) exponential stiffening, and (*vi*) a stick-slip plateau until failure. Figure modified from (Cranford et al., 2012; Tarakanova & Buehler, 2012).

Parameter	Value
Initial stiffness, E_1	875.9 MPa
Exponential parameter, α	14.2
Tangent stiffness parameter, β	180 MPa
Final stiffness, E_2	491.2 MPa
Yield strain, ε_y	0.1356
Softening strain, ε_s	0.6322

Ultimate (breaking) strain, ε_b	0.6725
Radial thread diameter (from (Alam, Wahab, & Jenkins, 2007; L.H. Lin & Sobek, 1998))	3.93 μm
Spiral thread diameter (from (Alam et al., 2007; L.H. Lin & Sobek, 1998))	2.40 μm

Table 2.1 | Atomistically derived dragline silk stress-strain behavior parameters. Radial and spiral thread diameters taken from experimental findings (Alam et al., 2007; L.H. Lin & Sobek, 1998). Table modified from (Cranford et al., 2012).

Constants C_1 and C_2 ensure continuity, where

$$C_1 = E_1\varepsilon_y - 1, \tag{5}$$

$$C_2 = \exp\left[\alpha\left(\varepsilon_s - \varepsilon_y\right)\right] + \beta\left(\varepsilon_s - \varepsilon_y\right) + C_1. \tag{6}$$

For tensile stretching, the stress-strain behaviour is converted to a force-displacement spring function, to allow a molecular dynamics implementation, given by:

$$F(r) = A_0 \cdot \sigma\left(\varepsilon(r)\right), \tag{7}$$

$$\varepsilon(r) = \frac{r - r_0}{r_0}, \tag{8}$$

such that

$$r_y = r_0(1 + \varepsilon_y), \tag{9}$$

$$r_s = r_0(1 + \varepsilon_s), \tag{10}$$

$$r_b = r_0(1 + \varepsilon_b). \tag{11}$$

The model is implemented by using a particle dynamics formulation, motivated by molecular dynamics, where the total energy of the web system (the energy between all the bonded pairs of particles) is defined as:

$$U_{\text{web}} = \sum_{\text{threads}} \phi_{\text{material}}. \tag{12}$$

The total energy of the web system is the sum of the elastic potentials of all threads, where ϕ_{material} refers to the constitutive energy expression. For dragline silk:

$$\phi_{radial}(r) \tag{13}$$
$$= A_0 \times \begin{cases} \frac{1}{2}\frac{E_1}{r_0}(r - r_0)^2, & r \le r_y \\ \frac{r_0}{\alpha}\exp\left[\frac{\alpha(r - r_y)}{r_0}\right] + \frac{1}{2}\frac{\beta}{r_0}(r - r_y)^2 + C_1(r - r_y) + C_3, & r_y \le r < r_s \\ \frac{1}{2}\frac{E_2}{r_0}(r - r_s)^2 + C_2(r - r_s) + C_4, & r_s \le r < r_b \\ 0, & r \ge r_b \end{cases}$$

Constants C_1 and C_2 are defined as before and the constants C_3 and C_4 ensure continuity between the linear and exponential regimes, where

$$C_3 = \frac{1}{2}\frac{E_1}{r_0}\left(r_y - r_0\right)^2 - \frac{r_0}{\alpha}, \tag{14}$$

$$C_4 = \frac{r_0}{\alpha}\exp\left[\frac{\alpha(r_s - r_y)}{r_0}\right] + \frac{1}{2}\frac{\beta}{r_0}\left(r_s - r_y\right)^2 + C_1\left(r_s - r_y\right) + C_3. \tag{15}$$

The model framework used here can be easily adapted for other species of spiders, associated silk properties, and web geometries.

Empirically parameterized capture silk

We use a computational approach to probe the effect of varying capture silk material behavior on the performance of the web, by systematically exploring material property trends representative of natural silk. The model permits controlled variation of capture silk properties to evaluate their effect on the response of the web upon loading. Web structure, size and loading conditions are controlled while a systematic variation of capture thread material properties is applied based on observed empirical data (Brook O. Swanson et al., 2007). Rather than predicting patterns and relationships grounded on observations of natural systems, evolutionary products are directly incorporated into the model.

We compare a series of material laws describing capture spiral behavior in the web, modeled after naturally observed spiral threads to reflect both the nonlinear elastic

behavior and ultimate values of strength and extensibility (**Figure 1.3**). The approximate material behavior of the threads, as well as the range of maximum strength and extensibility values considered is modeled after Swanson *et al.* (Brook O. Swanson et al., 2007).

The material behavior of the threads is implemented by a combination of atomistically derived and empirically parameterized models. Because radial thread behavior shows little variation across species compared to the material variation of spiral threads, (B. O. Swanson, Blackledge, Beltrán, & Hayashi, 2005; Brook O. Swanson et al., 2007) a single material law is used for radial threads across the models (**Figure 2.2**). It is parameterized from full atomistic simulations of major ampullate (MA) dragline spider silk (Sinan Keten & Markus J. Buehler, 2010; S. Keten & M.J. Buehler, 2010; Keten et al., 2010; Nova et al., 2010; van Beek, Hess, Vollrath, & Meier, 2002), and defined previously.

Six material laws are considered for capture spiral threads in the web model, to characterize the effect of extensibility-for-strength exchange observed in capture silk across different species of spiders (**Figure 1.3**) (Brook O. Swanson et al., 2007). An exponential material law is fitted to tensile experiments (Brook O. Swanson et al., 2007),

and kept consistent across the models to controllably observe the effect of strength and extensibility variation. The material law for spiral capture silk is modeled by:

$$\phi_{\text{spiral}}(r) = A_0 \times \begin{cases} r_0 a \exp\left[\frac{(r-r_0)}{r_0}\right] + \frac{1}{2} br(r-2r_0)/r_0 + rc\,, & r < r_b \\ 0\,, & r \geq r_b \end{cases}. \quad (16)$$

The spread of ultimate strength and strain values, $(\sigma_f, \varepsilon_f)$, for capture silk is based on observed silk material behavior variation across a series of spider species (**Figure 2.3**) (Brook O. Swanson et al., 2007). Critical values for the six material laws are listed in **Table 2.2**.The modulus at small deformation, E_i, is assumed to be 3 MPa for capture silk (J.M. Gosline et al., 1999). The ultimate strength and strain values of the silks define the constants in Equation (16) to be:

$$a = \frac{\sigma_f - E_i \varepsilon_f}{e^{\varepsilon_f} - \varepsilon_f - 1}, \quad (17)$$

$$b = E_i - a, \quad (18)$$

$$c = -a. \quad (19)$$

Model	Ultimate tensile strength (σ_t)	Ultimate tensile strain (ε_t)
1	1,200 MPa	1 mm/mm
2	1,000 MPa	2 mm/mm
3	800 MPa	3 mm/mm
4	600 MPa	4 mm/mm
5	400 MPa	5 mm/mm
6	200 MPa	6 mm/mm

Table 2.2 | Ultimate strength and strain parameters for the materials laws depicted for six spiral silk models in **Figure 2.3.**

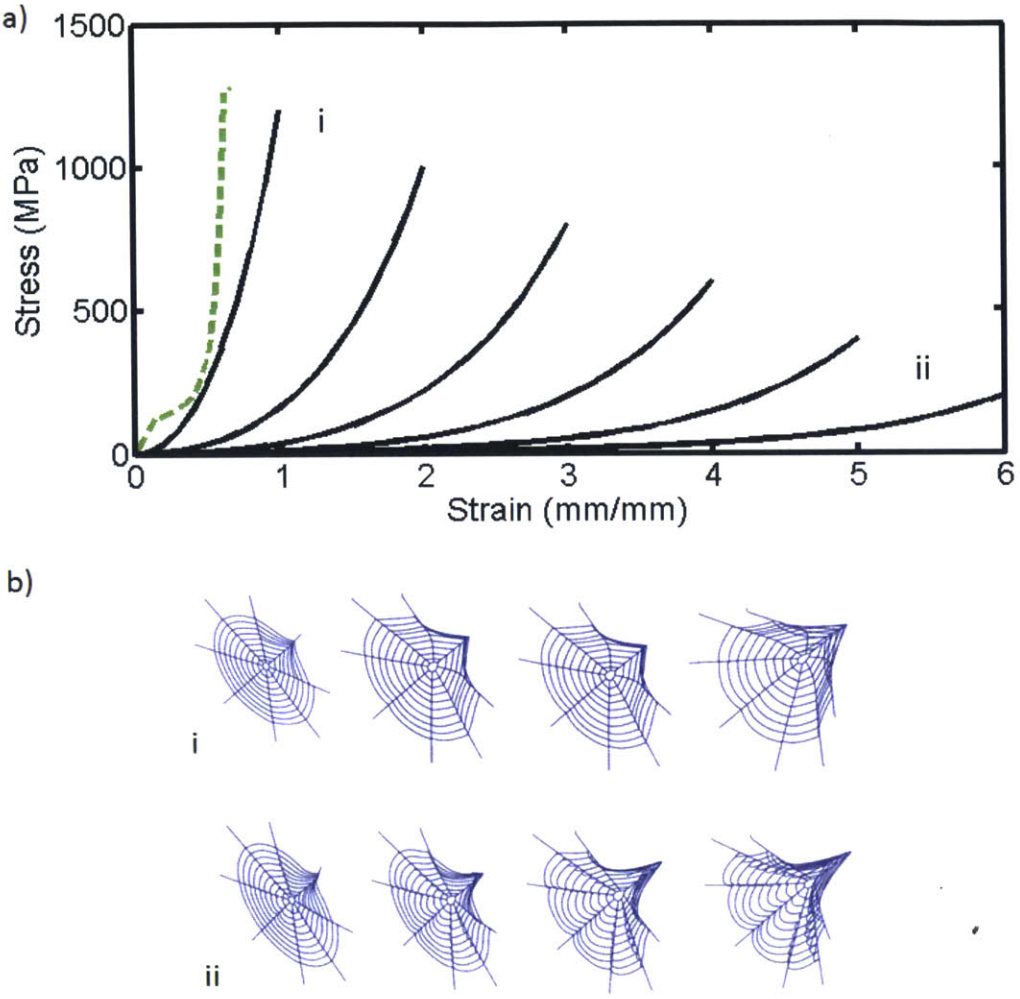

Figure 2.3 | a) Six material laws were used to model capture spiral threads in the web to characterize the effect of extensibility-for-strength exchange observed in spider capture silk (shown in black). Radial silk material behavior exhibited little variation across species and was consequently kept consistent across the models. The dotted green line represents the atomistically derived material behavior of dragline silk radial threads. The spread of maximum stress and strain values for capture silk is based on the observed silk material variation across spider species (**Figure 1.3**). b) Snapshots of the web corresponding to two extreme cases (labeled i, ii in a)). Figure modified from (Tarakanova & Buehler, 2012).

Application of Load - Steered Molecular Dynamics

Mechanical loading is applied to web models as illustrated in **Figure 2.4a** (loaded threads shown in red). A constant-velocity spring load (spring constant 0.007 N/m and constant velocity 0.002 m/s, resulting in an applied force of 0.000014 N/s) is applied to a segment of thread in the out-of-plane direction, incrementally until failure.

This loading scenario is meant to mimic the force experienced by the web upon impact of prey applied primarily at a right angle (Denny, 1976). Out-of-plane deflection and force are calculated. A sample force-displacement plot is presented in **Figure 2.4b**. Corresponding web deformation states are shown in **Figure 2.4c**, depicting a sample data set for quantifying energy absorption.

Energy Absorption

Web deformation and failure mechanics are quantified in the models by comparing the energy absorption capacity of the web. It has been suggested that among various strategies of energy dissipation, specifically, i) the internal energy dissipation by radial threads, ii) dissipation by spiral threads and iii) aerodynamic damping, radials play the most significant role in prey capture (A. T. Sensenig, Lorentz, Kelly, & Blackledge, 2012). Nevertheless, understanding how material behavior of the spirals affects energy

dissipation can elucidate the functional role spirals play in the web. Web performance is measured by the amount of energy that it can absorb. This energy is quantified as the area under the force-displacement curve of the web, shown in **Figure 2.4b,** as it is stretched by a spring-load, until failure, which is defined as the breaking point of the loaded threads.

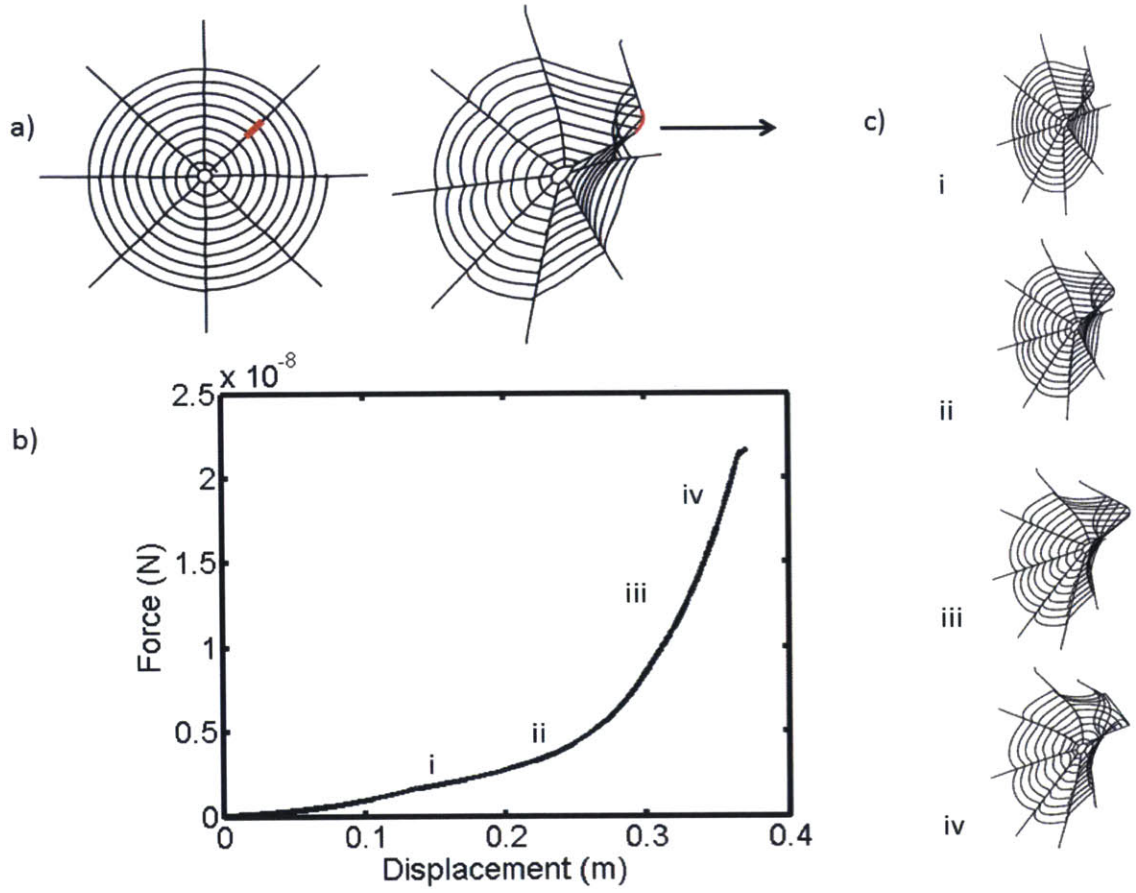

Figure 2.4 | (a) Constant-velocity force increments are applied to a radial thread segment (shown in red) to study web deformation behavior for various capture silk material properties. (b) Force–displacement data for a web pulled in the out-of-plane direction until failure. Numerals (i–iv) correspond to web deformation states as shown in (c). Figure modified from (Tarakanova & Buehler, 2012).

The kinetic energy of the prey can either be stored through elastic deformation of spiral and radial threads or it could be dissipated in the form of heat through friction as the web stretches (J.M. Gosline et al., 1999; L. H. Lin et al., 1995). So, more accurately, the energy we calculate includes both energy absorbed by elastic deformation and energy dissipated through friction. It has been shown in sequential loading and unloading experiments of real silk fibers that hysteresis in silk threads is about 65%, indicating that 65% of the kinetic energy is dissipated into heat upon impact (Denny, 1976; J.M. Gosline et al., 1999). The area "lost" to hysteresis corresponds to the energy dissipated through friction. So, when we refer to energy absorption capacity, we are in fact discussing the total energy associated with deformation, which is a combination of energy dissipated in the form of heat and the energy absorbed through elastic stretching. Friction is simulated by a damping force introduced in the model while elastic energy dissipated is governed by the formulation of the material behavior of the threads.

Simulation protocol and software

The simulations were performed using the massively parallelized modelling code LAMMPS (Plimpton, 1995) (http://lammps.sandia.gov/), modified to allow the constitutive behaviors describe. Web models are simulated using molecular dynamics formulations, with an *NVE* ensemble at finite temperature (300 K) (where N=constant

particle number, V=constant simulation volume, E=constant energy). A small damping force is introduced to dissipate kinetic energy (approximately 1 mN-s-m^{-1}) for all simulations. The web structure is minimized and equilibrated for 10 seconds (100,000 time steps) prior to the addition of any load. The calculations and analysis were carried out using a parallelelized LINUX cluster at MIT's Laboratory for Atomistic and Molecular Mechanics (LAMM). Visualization has been carried out using the Visual Molecular Dynamics (VMD) package (Humphrey, Dalke, & Schulten, 1996).

Results

Nano to Macro: Bridging Length Scales - Linking Building Blocks to Structure and Function

Silk's extraordinary properties on the macroscopic scale ultimately stem from the balance of strength and extensibility at the molecular scale. The balance between strength and extensibility is achieved through the combination of distinct secondary structure units in silk protein, where the interplay of the two constituent domains characterizes the nanoscale deformation mechanisms of the emerging nanocomposite structure.

This link is captured through the mechanical characterization of silk molecules and the orb web model. The orb web geometry upon which the model considered here is based is pictured in **Figure 3.1a.** A spring load at constant velocity is applied to a single radial thread mimicking the impact of prey striking the web or a piece of debris, until failure occurs, defined by the initial rupture of the loaded thread. Area of contact where the load is applied is shown in red in **Figure 3.1b**. The deformation proceeds for approximately three minutes (in real time) until the web breaks. The gradual application of load permits us to track the various molecular-level deformation regimes. **Figure 3.1c** displays the development of deformation states together with five representative snapshots of the web. Molecular deformations corresponding to deformed web states are shows in **Figure 3.2**.

The first web configuration corresponds to the initial application of load where little deformation of the web is visible (42 seconds). The deformation state of the whole radial thread is at zero, corresponding to compact protein constituent domains (as illustrated by the corresponding snapshot), where no unfolding has yet occurred. As the load is applied, the web stretches to its second configuration (83 seconds). The composing protein structure approaches the yield point when amorphous domains begin to unfold. As the amorphous domain unfolds, hydrogen bonds break and the beta turn content decreases. Beta turns within the amorphous domains provide hidden length, leading to

the great extensibility and toughness observed in silk. The source of this observation is an increased density of hydrogen bonds with increased turn formation. The following web configuration (125 seconds) corresponds to further unfolding of amorphous domains and the onset of rupture of hydrogen bonds within the domains. The fourth snapshot at 167 seconds describes a molecular phase where crystals begin to form and sustain the stress within the amorphous domains as chains are stretched to the limit. The final snapshot (176 seconds) is taken just before failure occurs. Failure comes in as hydrogen bonds break in the crystalline regions, which triggers the sliding of beta sheet strands. In parts of the loaded radial thread, beta-sheet nanocrystals begin to slip (indicated by the deformation states that reflect the surpassing of the dashed green line, marking the onset of stick-slip deformation). The coherent interaction among different domains (Nova et al., 2010) within the silk protein results in a nonlinear constituent behavior of silk, achieving high strengths from the stiff crystal components, and improved extensibility and toughness resultant from constituents of the amorphous region.

Experiments suggest that nanocrystal size, moderated by the reeling speed of the silk, gives silk its superior strength and toughness. Beta-sheet crystals act as stiff orderly crosslinks whose underlying chemical structure is defined by assemblies of hydrogen bonds, one of the weakest types of chemical bonds in Nature. These 'inferior' building

blocks together contribute to a structure that is essentially responsible for holding together the amorphous domains, reinforcing the polypeptide strands, and thus functioning as load-transferring units (Keten et al., 2010).

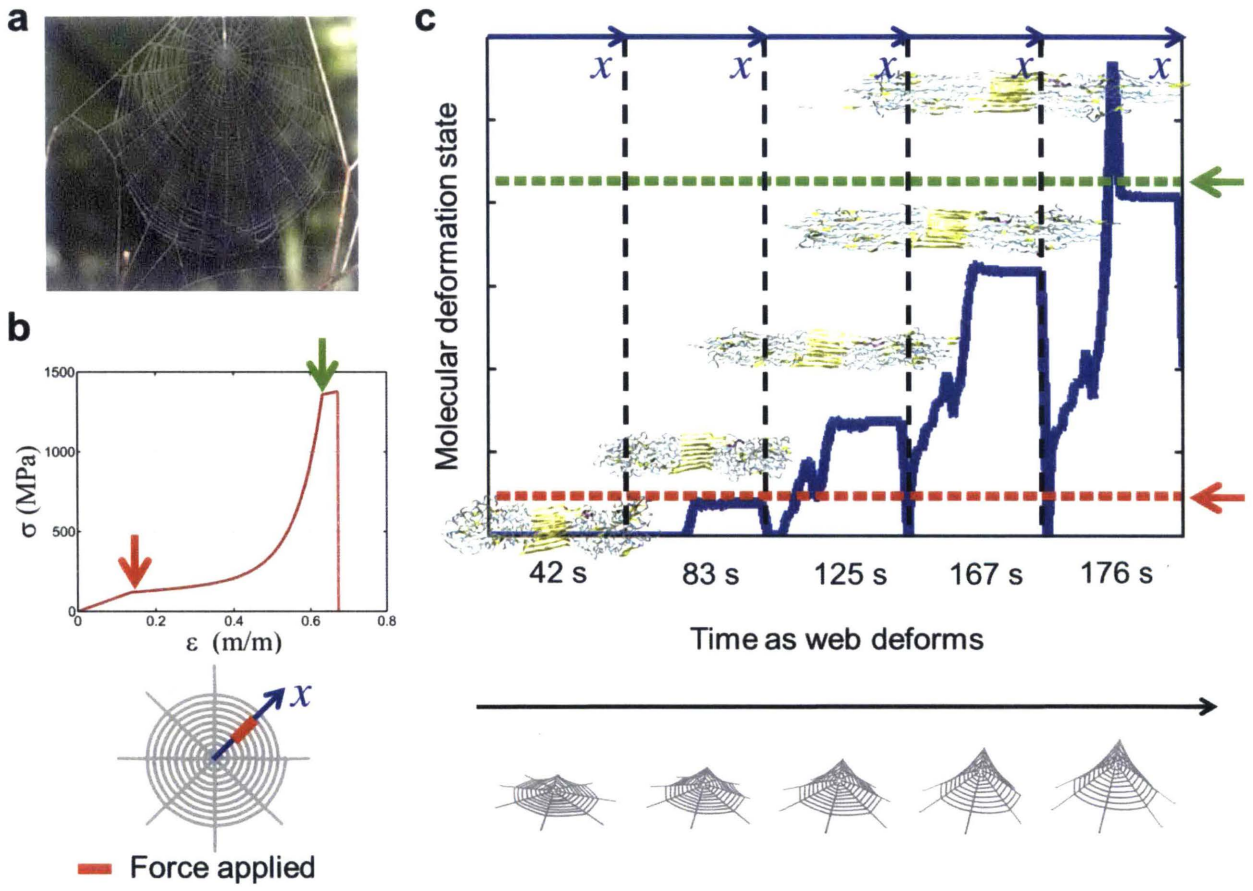

Figure 3.1| Mechanical behavior of dragline spider silk, and web response upon localized loading of radial thread. a, Geometry of typical spider orb-web, from *Cyclosa simplicicauda*. Image of the web reprinted with permission from Swanson *et al.* (Brook O. Swanson et al., 2007), copyright © 2001 by John Wiley and Sons. **b**, Threads in the web are modeled as particles connected via springs, exhibiting a stress-strain behavior parameterized from atomistic simulation of silk protein and as shown in the stress-strain plot (S. Keten & M. J. Buehler, 2010; S.W. Cranford 2011). The red arrow corresponds to the yield point, where amorphous domains

begin to unfold as hydrogen bonds break. The green arrow indicates the point at which beta sheet nanocrystals begin to exhibit stick-slip deformation. The deformation field in the thread shown in blue is plotted in panel **c**, also marking the thread where the local force is applied. **c**, Deformation fields in a radial thread, under web loading with a constant velocity of 0.002 m/s. The figure shows the molecular deformation state along the radial thread, depicted for five time steps (separated by dashed lines). The molecular deformation states correspond to the five snapshots of the web shown in the lower part of the plot (web deformation tracked from the onset of deformation to just prior to failure). The red and green dashed lines correspond to the deformation states at the yield point and onset of the stick-slip behavior of beta-sheet crystals, respectively. The snapshots of protein constituents correspond to the molecular conformations present within the loaded radial at each time step (enlarged view in **Figure 3.2**). The first time step corresponds to onset of stretching where the protein has not begun to unfold. At 83 seconds, the loaded amorphous regions within the protein domains of the loaded thread begin to stretch. At 125 seconds, continued unfolding is observed until crystals begin to form in the amorphous region at 167 seconds. At 176 seconds, just prior to failure, several loaded beads show a peak in the deformation state, corresponding to the regime of slipping beta-sheet crystals. Figure modified from (Tarakanova & Buehler, 2012).

Studies examining crystal size elucidate a further link between chemical composition and resultant signature behavior within silk (Du et al., 2006; Sinan Keten & Markus J. Buehler, 2010; S. Keten & M.J. Buehler, 2010; Keten et al., 2010). Smaller crystals exhibit superior properties up to a critical (optimal) size of 2-4 nm, as a result of the difference in deformation mechanism on the molecular scale. In small crystals, a stick-slip motion is observed as hydrogen bonds brake and reform. The self-healing ability of smaller crystals owing to the continuous reformation of hydrogen bonds protects the crystals

from catastrophic failure as hydrogen bonds are shielded from exposure to water which facilitates rupture. In contrast to soft and brittle larger crystals which fail catastrophically by crack-flaw formation and consequent bending, smaller crystals exhibited shear deformation. The effective capacity of hydrogen bonds to resist failure by self-healing in conjunction with nanoconfinement at the crystal scale results in strong, stiff crystals of characteristic size, as verified experimentally (Du et al., 2006; Keten et al., 2010).

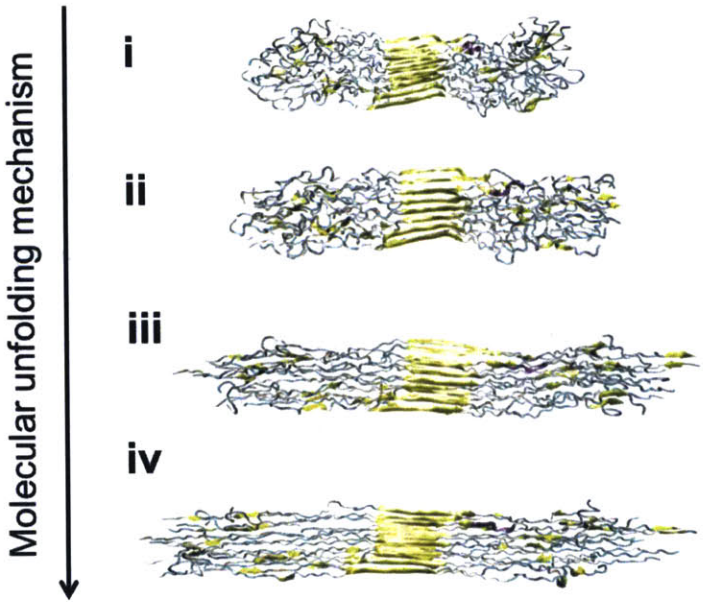

Figure 3.2: Molecular unfolding mechanism of the silk protein nanocomposite. Qualification of the four stage deformation mechanism of a single silk repeat unit. Initially (i), the protein nanocomposite consists of coiled semi-amorphous domains exhibiting hidden length (shown in blue), embedding a stiff beta-sheet crystal (shown in yellow). As the protein begins to unfold (ii), amorphous domains unravel, revealing their hidden length. As the amorphous domains

stretch, new hydrogen bonds are created and beta crystal units begin to form within the amorphous domains, sustaining the stress on the system as amorphous regions are extended to their limit (iii). A final regime is observed as covalent bond rupture forces many hydrogen bonds to break rapidly within the amorphous domains (iv), initiating sliding of beta strands which ultimately leads to failure. Figure modified from (Tarakanova & Buehler, 2012).

Material links in failure mitigation

By linking molecular deformation regimes to web deformation states, the mechanism of web deformation and failure can be further elucidated. In fact, it is the molecular deformation mechanisms at the web scale that are responsible for the ability of the web to sustain load and resist catastrophic failure through a sacrificial mechanism (S.W. Cranford 2011). In such compliant structures, it is anticipated that the stiffest elements resist the greatest load (**Figure 3.3**).

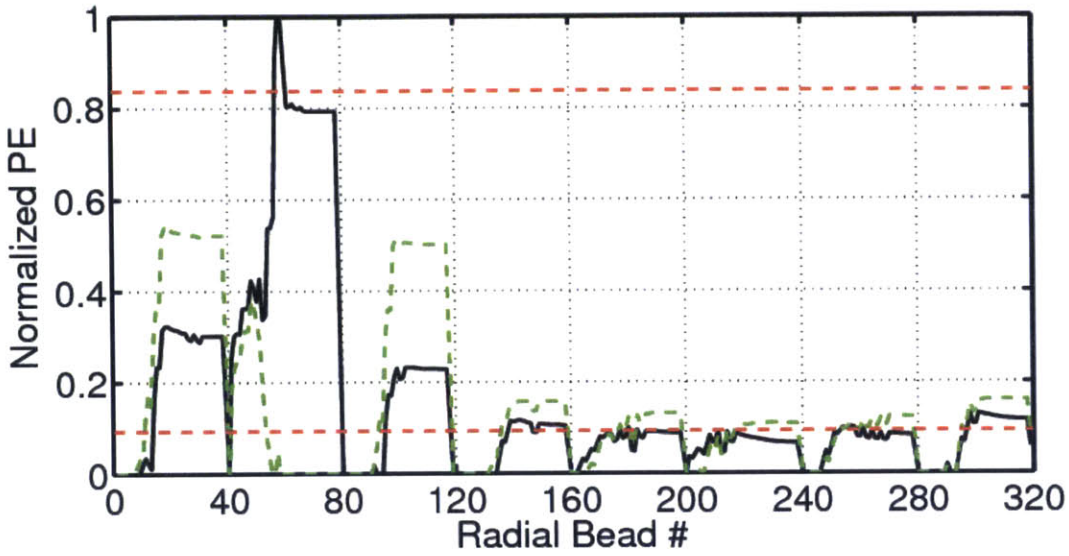

Figure 3.3 | The potential energy (PE) distribution for atomistically derived silk behaviour in radial threads. Energy is normalized with respect to maximum potential energy at failure. Stress is localized on the radial thread where load is applied directly (bead number 40 through 80). Figure modified from (Cranford et al., 2012).

The cooperative action of a stiffening structural member (the radial silk thread under load) with yielding (or softening) of ancillary members results in a localization of elastic resistance. Concurrently, adjacent radials reveal a partially stiffened state – immediately after failure, load is redistributed between these two adjacent threads, keeping the rest of the web intact and functional. The radial thread where load is applied incurs severe stiffening, while sections of the web removed from loading undergo limited deformation and strain.

In comparison to other common engineering materials, for example, linear-elastic and elastic-perfectly-plastic materials, the characteristic softening of silk at the yield point followed by stiffening at large strain is responsible for localization of damage in a loaded web. This has significant evolutionary implications, (B. O. Swanson et al., 2009; Fritz Vollrath & Selden, 2007) ensuring that debris or prey too large for the web to support will not cause irreparable damage, costing the spider energy to rebuild. Furthermore, the regulation of damage through control of material behavior has implications beyond webs to any structural design which would benefit from contained damage. Looking forward, the entirety of a bottom-up design paradigm illustrated here, where function can be manipulated through alteration of structure on different hierarchical scales, presents opportunities in design of enhanced and novel synthetic, biomimetic and biological materials that provide a wide array of material function at low weight.

Evolutionary Lessons From Spider Web Mechanics

To capture the variation in energy-absorption capabilities of a web due exclusively to fluctuation in capture silk material behavior, six material laws were considered, shown in **Figure 2.3a**, representing the observed trend in capture thread material through evolutionary time (Brook O. Swanson et al., 2007). Each model was identically

deformed to track the force-displacement behavior and the energy absorbed. Loading regions surrounding both spiral and radial threads were considered, as well as regions close to and far away from the hub (**Figure 3.5**). Results for the loading scenario shown in **Figure 2.4** are presented in **Figure 3.4.**

Energy absorbed by the web and toughness of individual capture silk fibers is shown in **Figure 3.4a.** Toughness of thread fibers was calculated as the area under the stress-strain curve used to parameterize individual threads in the web models. A peak in thread toughness is observed at a balance of strength and extensibility, where $(\sigma_f, \varepsilon_f) = (800\ \text{MPa}, 3\ \text{mm/mm})$. Contrary to expectation, energy absorption of the web steadily decreases as extensibility replaces strength in the fibers of the capture silk, even as toughness of the individual fibers peaks. The maximum force and displacement of the web prior to breaking is captured in **Figure 3.4b** and **c** for the corresponding material law models from **Figure 2.3a**.

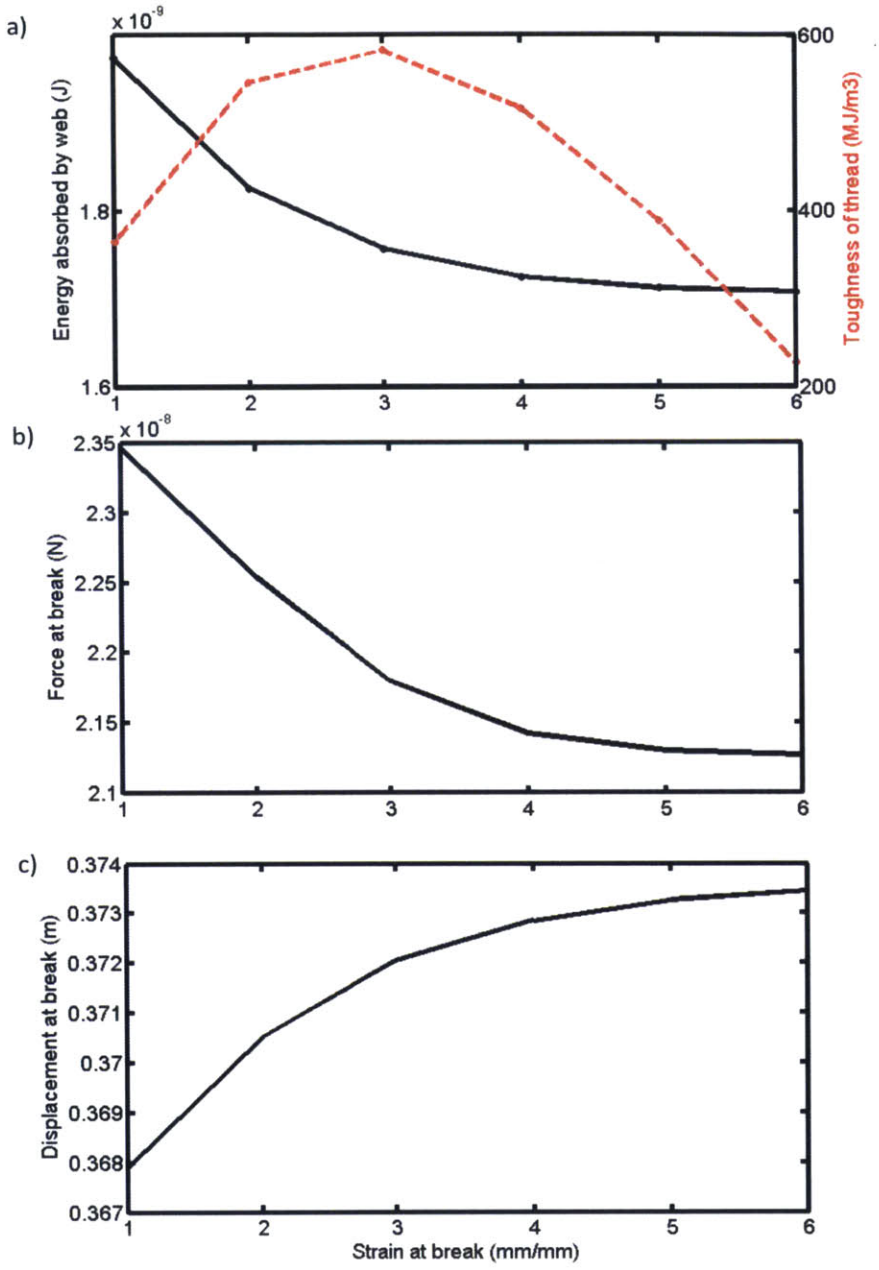

Figure 3.4 | Energy absorption, toughness and other mechanical properties of the web. a) Energy absorbed by the web (defined as the area under the force-displacement curve) and the corresponding capture thread toughness (defined as the area under the stress-strain curve for a single spiral thread); b) force of the web at break; and c) displacement of the web at break compared for six material laws shown in **Figure 2.3a**. Figure modified from (Tarakanova & Buehler, 2012).

The force to break the web decreases with decreased capture thread strength while maximum extension of the web increases with increased capture thread extensibility, as expected. Energy absorbed by the web is determined both by the maximum force required to break the web and by the ultimate extension the web can reach before breaking. We attribute the surprising finding that energy-absorption capacity decreases with increasing capture thread extensibility, even as thread toughness peaks, to the fact that the force required to break the web must be the dominating factor determining web performance.

Three additional loading scenarios are considered and the web is found to behave in a similar manner (**Figure 3.5**).

We conclude that the *mechanism of deformation* that appears in webs made of viscid capture silk, rather than the overall ability of these webs to absorb energy, is more significant to the observed success of viscid capture silk. The difference in energy dissipation mechanisms between the two spider super families has been observed previously by Kohler *et al.* (Kohler & Vollrath, 1995). In this study we find that the mechanism of web deformation may be more relevant to spider diversification than the ability of the web to absorb more energy upon deformation.

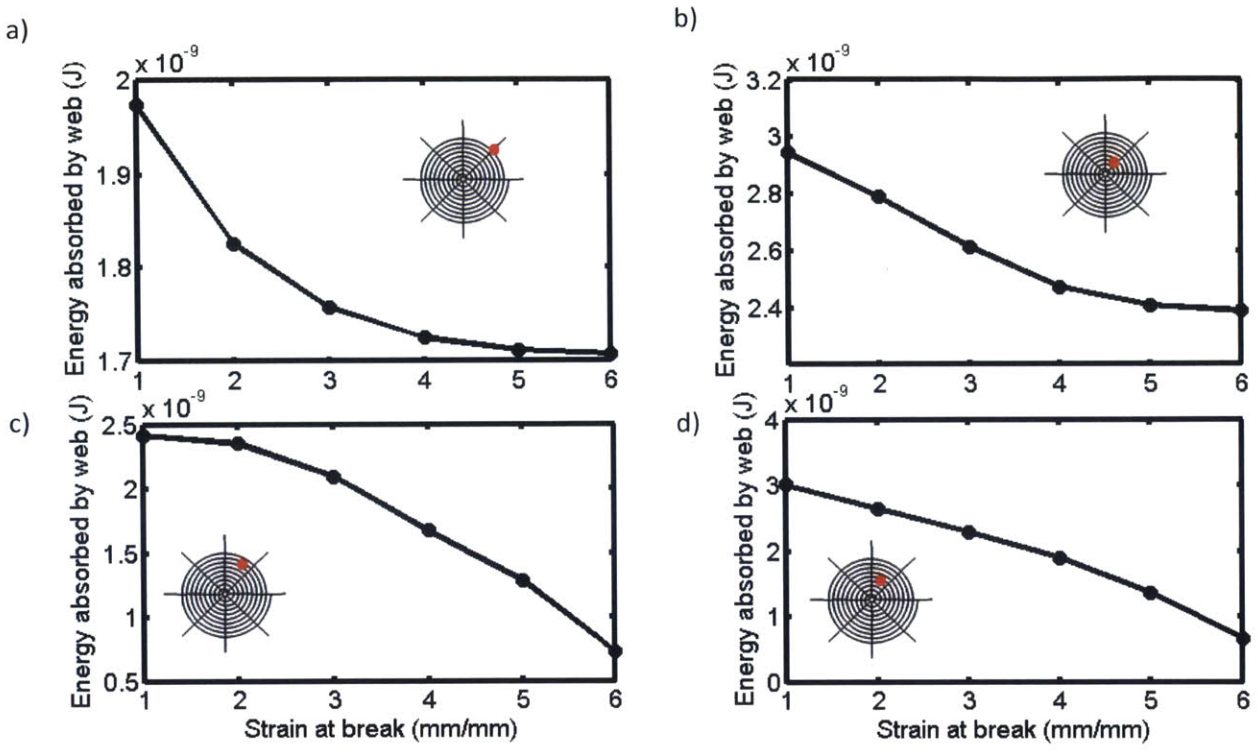

Figure 3.5| Energy absorption for varied spiral thread material laws (as in **Figure 2.3a**) under different loading conditions. Loaded regions are indicated in red: a) radially-centered, far from hub; b) radially-centered, close to hub; c) spiral-centered, far from hub; d) spiral-centered, close to hub. All loading scenarios show decreased energy absorption for the given material trend. Loading scenario in a) is considered throughout the body of the paper. Figure modified from (Tarakanova & Buehler, 2012).

Web deformation is captured explicitly for two representative web models in **Figure 2.3b**, comparing two limiting cases: (i) strong spiral threads exhibiting minimal extension and (ii) weak, extensible spiral threads. Snapshots of the web under deformation show that for the stronger, less extensible spiral threads (i), the web extends as an umbrella, where spiral threads act cooperatively with radials causing a more global deformation, as a result of a similar material law defining radial and spiral

thread mechanics. Weaker, more extensible spirals (ii) have a greater effect on the web's deformation mechanism as they are more engaged in full-structure deformation, resulting in localization. This achieves more extensibility, however, because deformation is governed by the weaker spirals in this case, the total energy absorption capacity is reduced. The wide diversification of araneoid spiders implies that even with a reduced capability to absorb and dissipate energy, the mechanism of web deformation through extension is advantageous in prey capture.

Our rather surprising observation that viscid capture silk in the web results in lower energy dissipation also implies that capture threads in araneoids play a weaker prey-catching function, as has been suggested in a recent study by Sensenig *et al.* (A. T. Sensenig et al., 2012). We propose that the *mechanism* of prey capture in the orb is more important from the evolutionary stand point of capture silk than the web's total dissipative capacity.

Previously, we compared the mechanical response of a loaded web composed of threads with varying material laws (Cranford et al., 2012). In particular, we found that a web composed of natural silk with a characteristic nonlinear material law was more robust and damage-tolerant than a web made of threads with material laws mimicking standard engineering materials with a stiffer initial regime upon deformation. Similarly,

the more elastic viscid silk compared favorably against stiffer cribellate silk. One reason for this may be minimization of damage to the web in case of mechanical failure. If the web breaks, we observe that damage is more localized, so it is more economical for the spider to rebuild. Hence the reduced energy dissipation capacity observed for weaker capture threads may be counterbalanced by the conservation of metabolic energy used to restore damaged regions. Effectively, the capture threads adopt a new function in the web: they optimize the spider's energy primarily by improving the web's structural mechanics rather than by optimizing the size of the captured prey.

This observation may also shed light on the role of capture silk in prey retention after it has been intercepted by the web. In webs made of viscid capture silk, prey is retained by sticking to the aqueous glue droplets coating the threads, which cling to the prey as it struggles to escape. Previous studies have discussed the importance of web geometry and close alignment of spiral threads for engulfing the struggling prey as it adheres to adjacent threads (Blackledge, Kuntner, & Agnarsson, 2011). The increased elasticity of capture thread plays an important role in dissipating kinetic energy of the prey upon recoil. We propose that in addition to serving a dissipative function as the prey oscillates in the web, more elastic capture silk keeps the prey in a contained region of the web, forcing it to attach to adjacent threads more efficiently.

To systematically compare the effect of capture silk material variation on web mechanics, 24 material laws were studied, spanning the full spectrum of experimentally observed capture silk material laws (**Figure 3.6**).

Again, four loading scenarios were considered, illustrated in **Figure 3.5.** The effect of increasing thread extensibility for a constant thread strength (**Figure 3.6a**) as well as the effect of varying strength at a constant extensibility (**Figure 3.6c**) was evaluated. The effect of increasing thread extensibility for a given strength value is comparable to the effect of increasing extensibility while at the same time decreasing strength. Energy absorption decreases with increasing thread extensibility, because deformation becomes primarily governed by the weaker spiral threads. A similar loading scenario, but closer to the hub of the web, yielded a similar result (**Figure 3.7**).

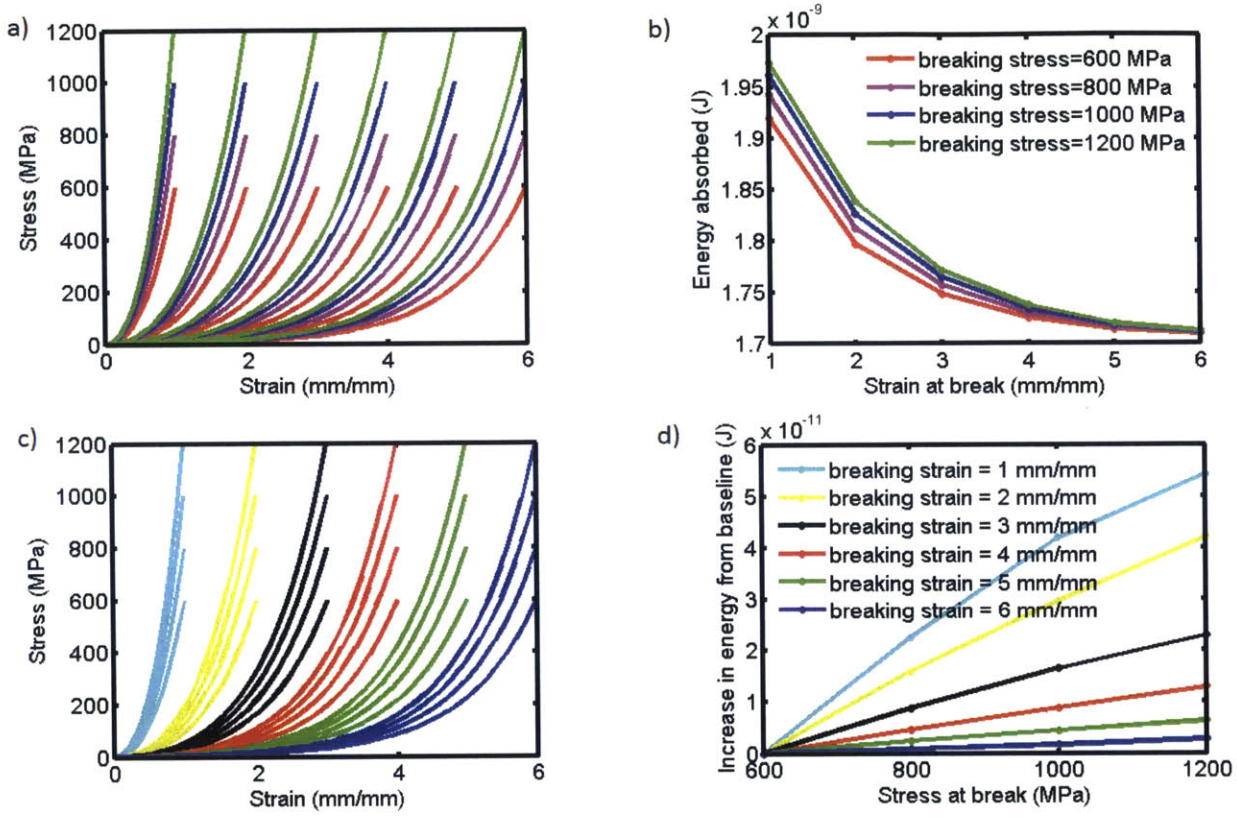

Figure 3.6 | Effect on web performance due to variation in capture silk properties. a) Summary of 24 material laws used for parameterizing capture silk in web models. Material laws are color-coded showing a trend of increasing extensibility for a given thread strength. b) Energy absorbed by the web under loading conditions shown in **Figure 3.5a** is recorded for each model. c) The same 24 material laws are shown, colored to display a trend of increasing strength for a given thread extensibility. d) The effect on energy absorption in the web when increasing the strength of the material while keeping extensibility constant for six different breaking strains shown in c). Baseline energy absorption is defined as the energy absorbed for breaking stress of 600 MPa for a set of material laws at a given breaking strain. Figure modified from (Tarakanova & Buehler, 2012).

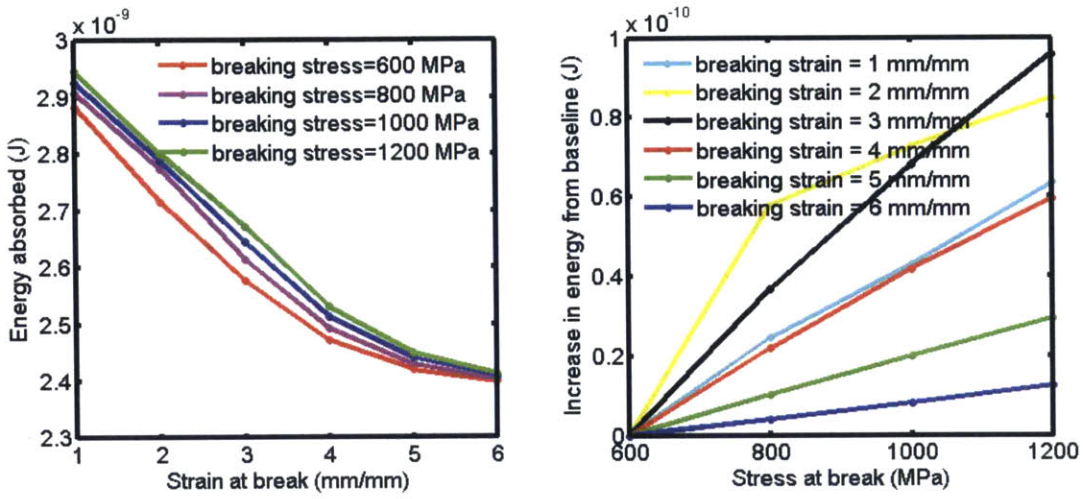

Figure 3.7| a) Total energy absorption by the web for the loading scenario in **Figure 3.5b** (radially-centered, close to hub) and b) increase from baseline value in total energy absorbed, corresponding to material trends in **Figure 3.6a** and **c,** respectively. Figure modified from (Tarakanova & Buehler, 2012).

Spiral thread loading was considered for comparison, but we found that, as a result of the highly variant mechanical properties between spiral and radial threads, loading of spirals resulted in very localized failure of the loaded thread and the web's energy absorption was therefore governed by the mechanical properties of the spiral threads alone (**Figure 3.8**).

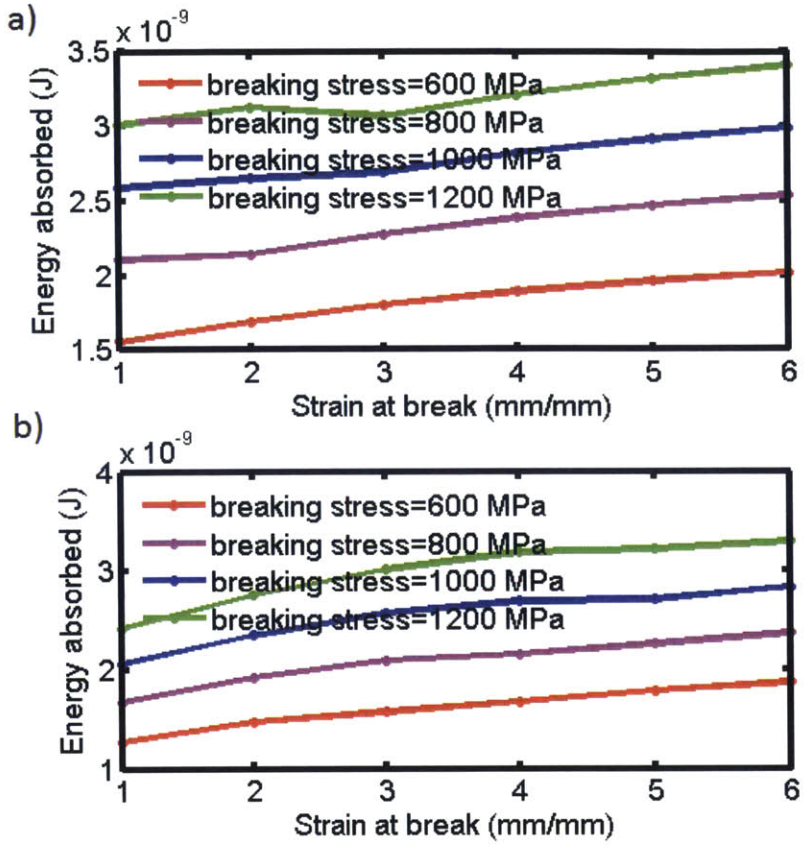

Figure 3.8| Total energy absorption of the web for varied spiral thread material laws shown in **Figure 2.3a** for a) spiral-centered, close to hub loading and b) spiral-centered, far from hub loading. Figure modified from (Tarakanova & Buehler, 2012).

When extensibility is held constant for a set of strength values, as in **Figure 3.6c**, an interesting trend is observed. As threads become more extensible, the ultimate strength of the thread has an increasingly reduced effect on web performance, quantified by the web's energy-absorption capacity. For instance, the energy absorbed in webs with $(\sigma_f, \varepsilon_f) = (600\ \text{MPa}, 6\ \text{mm/mm}\ )$ and $(1200\ \text{MPa}, 6\ \text{mm/mm})$ is approximately equal,

while the difference is much more pronounced between webs with $(\sigma_f, \varepsilon_f) = (600\ \text{MPa}, 1\ \text{mm/mm})$ and $(1200\ \text{MPa}, 1\ \text{mm/mm})$ (**Figure 3.6d**). Loading closer to the hub results in a similar trend (**Figure 3.7b**). This gives a direct mechanistic insight into the material "trade-off" observed in the evolution of webs: more extensible threads do not need strength to provide a particular function in a full web structure, as deformation is governed by extensibility. For a large thread extensibility, strength plays an insignificant role in improving energy dissipation capacity. Therefore, more extensible, weaker threads can achieve the same effect and thereby reduce associated production costs for the spider. So, to the extent that spiral thread contributes to prey capture, the spider optimizes cost effectiveness by making weaker threads which achieve the same functional role.

These findings suggest that the key for the observed evolutionary trade-off between strength and extensibility of spirals is not primarily a result of improved energy absorption capacity in more extensible webs. Rather, it is a combination of at least two factors. First of all, more extensible, weaker threads, representative of viscid capture silk, result in increased and highly localized deformation of the web structure. This method of energy dissipation- through elastic deformation- functions in arresting quick flying prey. The evolution of viscid capture silk is tied to a different mechanism of dissipating energy rather than to net total energy dissipation. This may be

advantageous from a structural point of view-as a source of minimizing damage should it occur, and from the prey-capture perspective- as web extension localizes prey upon impact, easing capture. Secondly, as threads become more extensible, less strength is needed to achieve the same effective energy dissipation response in the web - an additional metabolic advantage with respect to energy conservation.

We note that because our study considers variation in spiral threads only, it may be offset in natural systems by parallel changes in radial thread diversification, although variation in radial threads is generally much less significant than in spirals (B. O. Swanson et al., 2005). However, our goal is to understand the mechanistic effect on the web's response resultant from variation of spiral thread material behavior exclusively, as this trend is most striking and largely unexplored across species. We show that the observed trade-off is not only behaviorally and energetically advantageous for the spider, but mechanically optimized. As the thread becomes more extensible, it needs less strength to absorb equivalent amounts of energy. In other words, ultimate strength of the spiral threads has a reduced effect on the behavior of the web system as threads become more elastic.

Various complementary studies have tried to explain the success of viscid capture silk and its role in the evolution of the orb web (Blackledge & Hayashi, 2006; Blackledge et

al., 2009; Bond & Opell, 1998; Opell, 1998, 1999; B. O. Swanson et al., 2009; Fritz Vollrath & Selden, 2007). Now, we can add to the list the mechanical benefits of the observed trade-off between strength and extensibility, demonstrative of the shift from cribellate to viscid capture silk: viscid capture silk is beneficial for minimizing energetic costs associated with orb creation, helps to reduce damage under extreme loads and retains prey by localizing it in the web.

Overview, Implications and Future Outlook

We have outlined a series of previous models describing increasing levels of hierarchy within a spider web, and illustrated how multiscale modeling complements experimental efforts in developing a thorough understanding of the mechanics of a spider's web. The strength of each model lies in its catalytic nature. In chemistry, a catalyst functions to speed up reaction rates, bridging the reactant and product states in solution. In hierarchical modeling of materials, the model allows for a convenient link between length scales, bridging scales by pinpointing assembly and deformation mechanisms. At the molecular level, the model takes in as input the sequence of residues, yielding structure, size characterization and material behavior parameters and mechanisms as output. The amino acid sequence dictates the chemistry of higher-order secondary protein structures of silk: domains of low and high density of hydrogen

bonding, for instance. Low-density hydrogen bonding is present in the coiled, elastic domains while denser hydrogen bonding results in the mechanism of nanoconfinement, which directs the characteristic size and strength of crystals composing silk. The two domains establish a collaborative interaction contributing complementary function: strength and extensibility. The unique advantage of the bottom-up analytic approach is, in addition to a more complete and accurate system description, the potential to link higher order scales to fundamental components at lowest hierarchical levels.

We propose that through analyzing bridging hierarchies within complex materials, material scientists will be able to narrow the knowledge gap that exists in the description of materials. We envision that such a scale-bridging approach to studying hierarchical materials, including materials other than silk such as natural and synthetic fibers, will facilitate a better understanding at all levels of material composition and provide tools for effectively manipulating these properties to achieve superior material qualities for application in a variety of fields, from structural engineering to medicine. As the understanding gap narrows, we seek direct methods to implement mutability into materials at all length scales.

The coarse-grained spider web model is a culmination of a series of multi-scale structural spider silk models completed in the Buehler group over the years. From this

perspective, we have described the interplay of material and structure within the hierarchy of material scales.

In this thesis, we look beyond a materials-level analysis of the spider web, to focus on the evolutionary implications. We target a well-characterized evolutionary trend found in the capture silk material behavior across different orb-weaving spider species through evolutionary time. By integrating the multiscale modeling approach with evolutionary theory, we devise an evolution-material-structure-function feedback loop.

Orb-weaving spiders found today belong in two spider superfamilies, the Araneoidea and Deinopoidea (Griswold et al., 1998). Between these superfamilies, capture silk material variation has been well documented: capture silks in the Deinopoidea superfamily tend to have higher ultimate stresses and lower ultimate strains than capture silks found in the Araneoidea superfamily (Brook O. Swanson et al., 2007). This material "trade-off" correlates with an apparent evolutionary advantage attributed to araneoids. Deinopoids use cribellate silk, the evolutionarily more primitive capture silk (Blackledge & Hayashi, 2006; W. Eberhard & Pereira, 1993; Garb et al., 2006; Opell, 1994), while araneoids use stretchy flagelliform silk (Peters, 1995; Tillinghast et al., 1993; F. Vollrath et al., 1990; F. Vollrath & Tillinghast, 1991). Araneoids are significantly more

diverse and can therefore be qualified as being evolutionarily "superior" to their sister deinopoid counterparts.

Many studies have addressed the question of divergence between the two superfamilies to understand the evolutionary advantage of the Araneoidea. Silk sequence, composition and structure; spider size and spinning behavior; orb-web architecture and orientation have all been implicated as factors for the differences between these two groups (Blackledge & Hayashi, 2006; Blackledge et al., 2009; Opell, 1997, 1998, 1999; B. O. Swanson et al., 2009; Fritz Vollrath & Selden, 2007). Several authors studied the question of evolutionary divergence by considering the mechanics of the webs, specifically the relationship between material variation and energy absorptive capacity of webs (C. L. Craig, 1987; Kohler & Vollrath, 1995; L. H. Lin et al., 1995; A. Sensenig et al., 2010).

In this thesis, we test the hypothesis that the observed material behavior shift, from stronger, less extensible threads in deinopoids to weaker more extensible threads in araneoids, is responsible for araneoids' proposed ability to absorb and dissipate energy better than their common ancestor with the more primitive deinopoids. In contrast to previous studies, we use an inverse approach to evolution by inputting material laws

for varied types of silk into a single web model, to controllably connect material behavior to higher order function in the web.

We identify that the cooperative effect of threads in the orb web plays a major role in determining web function and needs to be considered when evaluating evolutionary trends in material behavior of individual fibers. The two primary findings of this study are as follows: first, by systematically varying material behavior of capture silk within the web model, we find that the governing evolutionary principle from the mechanical standpoint is the *mechanism* of deformation rather than an increased energy absorption capacity. The reduced energy absorption capacity in weaker, more extensible araneoid-like threads can be linked to the effective deformation mechanism dominated by weaker spirals. We explain this observation in light of an increased damage tolerance and better prey retention capability.

The second contribution of this study is the finding that more extensible spiral threads require minimal strength for optimized effect. In defining web performance, extensibility dominates over strength in capture silk, as the effect of strength is progressively reduced when extensibility is increased. These results suggest that the effective prey capture mechanism is tied to a "less expensive" metabolic process for

making silk, allowing the spider to conserve energy by producing weaker but equally functional fibers.

This approach may be instrumental in understanding the evolution of hierarchical structures and it may be applied more broadly to study evolutionary shifts by simulating modifications not only in material behavior, but also in other factors, such as environmental conditions or system structure. Furthermore, these findings suggest that the material shift naturally derived through evolutionary mechanisms in spider silk may be employed more generally in engineered heterogeneous materials requiring conservation of phases contributing to material strength. We propose that natural structures provide an excellent material template for biomimetic, synthetic materials: the evolutionary process may provide insights into smarter modification of existing materials.

References

Agnarsson, I., Kunter, M., & Blackledge, T. A. (2010). Bioprospecting finds the toughest biological material: extraordinary silk from a giant riverine orb spider. *Plos One, 5*. doi: 10.1371/journal.pone.0011234.t001

Alam, M. S., Wahab, M. A., & Jenkins, C. H. (2007). Mechanics in naturally compliant structures. *Mechanics of Materials, 39*(2), 145-160.

Ayoub, N. A., Garb, J. E., Tinghitella, R. M., Collin, M. A., & Hayashi, C. Y. (2007). Blueprint for a High-Performance Biomaterial: Full-Length Spider Dragline Silk Genes. *Plos One, 2*(6), e514. doi: 10.1371/journal.pone.0000514

Blackledge, T. A., & Hayashi, C. Y. (2006). Unraveling the mechanical properties of composite silk threads spun by cribellate orb-weaving spiders. *Journal of Experimental Biology, 209*(16), 3131-3140. doi: Doi 10.1242/Jeb.02327

Blackledge, T. A., Kuntner, M., & Agnarsson, I. (2011). The Form and Function of Spider Orb Webs: Evolution from Silk to Ecosystems. *Advances in Insect Physiology, Vol 41: Spider Physiology and Behaviour - Behaviour, 41*, 175-262. doi: Doi 10.1016/B978-0-12-415919-8.00004-5

Blackledge, T. A., Scharff, N., Coddington, J. A., Szuts, T., Wenzel, J. W., Hayashi, C. Y., & Agnarsson, I. (2009). Reconstructing web evolution and spider diversification in the molecular era. *Proc Natl Acad Sci U S A, 106*(13), 5229-5234. doi: DOI 10.1073/pnas.0901377106

Bond, J. E., & Opell, B. D. (1998). Testing adaptive radiation and key innovation hypotheses in spiders. *Evolution, 52*(2), 403-414.

Boutry, C., & Blackledge, T. A. (2008). The common house spider alters the material and mechanical properties of cobweb silk in response to different prey. *J Exp Zool A Ecol Genet Physiol, 309*(9), 542-552. doi: 10.1002/jez.487

Buehler, M. J. (2010). Tu(r)ning weakness to strength. *Nano Today, 5*(5), 379-383. doi: DOI 10.1016/j.nantod.2010.08.001

Buehler, M. J., & Yung, Y. C. (2009). Deformation and failure of protein materials in physiologically extreme conditions and disease. *Nat Mater, 8*(3), 175-188. doi: 10.1038/nmat2387

Coddington, J. (1982). Monophyletic Origin of Orb-Webs. *American Zoologist, 22*(4), 886-886.

Coddington, J. A., Giribet, G., Harvey, M. S., Prendini, L., & Walter, D. E. (2004). Arachnida. *Assembling the Tree of Life*, 296-318.

Coddington, J. A., & Levi, H. W. (1991). Systematics and Evolution of Spiders (Araneae). *Annual Review of Ecology and Systematics, 22*, 565-592.

Craig, C., & Brunetta, L. (2010). *Spider Silk: Evolution and 400 Million Years of Spinning, Waiting, Snagging, and Mating* (1st ed. ed.): Yale University Press.

Craig, C. L. (1987). The Ecological and Evolutionary Interdependence between Web Architecture and Web Silk Spun by Orb Web Weaving Spiders. *Biological Journal of the Linnean Society, 30*(2), 135-162.

Craig, C. L., Riekel, C., Herberstein, M. E., Weber, R. S., Kaplan, D., & Pierce, N. E. (2000). Evidence for diet effects on the composition of silk proteins produced by spiders. *Mol Biol Evol, 17*(12), 1904-1913.

Cranford, S., Tarakanova, A., Pugno, N. M., & Buehler, M. J. (2012). Nonlinear material behaviour of spider silk yields robust webs. *Nature, 482*, 72-76.

Denny, M. (1976). Physical-Properties of Spiders Silk and Their Role in Design of Orb-Webs. *Journal of Experimental Biology, 65*(2), 483-506.

Du, N., Liu, X. Y., Narayanan, J., Li, L., Lim, M. L., & Li, D. (2006). Design of superior spider silk: from nanostructure to mechanical properties. *Biophys J, 91*(12), 4528-4535. doi: 10.1529/biophysj.106.089144

Eberhard, W., & Pereira, F. (1993). Ultrastructure of Cribellate Silk of 9 Species in 8 Families and Possible Taxonomic Implications (Araneae, Amaurobiidae, Deinopidae, Desidae, Dictynidae, Filistatidae, Hypochilidae, Stiphidiidae, Tengellidae). *Journal of Arachnology, 21*(3), 161-174.

Eberhard, W. G. (1989). Effects of orb-web orientation and spider size on prey retention. *Bull . British Arachnol. Soc, 8*, 45-48.

Garb, J. E., DiMauro, T., Vo, V., & Hayashi, C. Y. (2006). Silk genes support the single origin of orb webs. *Science, 312*(5781), 1762-1762. doi: DOI 10.1126/science.1127946

Garb, J. E., & Hayashi, C. Y. (2005). Modular evolution of egg case silk genes across orb-weaving spider superfamilies. *Proc Natl Acad Sci U S A, 102*(32), 11379-11384. doi: 10.1073/pnas.0502473102

Gosline, J. M., Demont, M. E., & Denny, M. W. (1986). The Structure and Properties of Spider Silk. *Endeavour, 10*(1), 37-43.

Gosline, J. M., Guerette, P. A., Ortlepp, C. S., & Savage, K. N. (1999). The mechanical design of spider silks: from fibroin sequence to mechanical function. *J Exp Biol, 202*(Pt 23), 3295-3303.

Gosline, J. M., Guerette, P. A., Ortlepp, C. S., & Savage, K. N. (1999). The mechanical design of spider silks: From fibroin sequence to mechanical function. *Journal of Experimental Biology, 202*, 3295-3303.

Griswold, C. E., Coddington, J. A., Hormiga, G., & Scharff, N. (1998). Phylogeny of the orb-web building spiders (Araneae, Orbiculariae : Deinopoidea, Araneoidea). *Zoological Journal of the Linnean Society, 123*(1), 1-99.

Guerette, P. A., Ginzinger, D. G., Weber, B. H., & Gosline, J. M. (1996). Silk properties determined by gland-specific expression of a spider fibroin gene family. *Science, 272*(5258), 112-115.

Guerette, P. A., Ginzinger, D. G., Weber, B. H. F., & Gosline, J. M. (1996). Silk properties determined by gland-specific expression of a spider fibroin gene family. *Science, 272*(5258), 112-115. doi: DOI 10.1126/science.272.5258.112

Harmer, A. M. T., Blackledge, T. A., Madin, J. S., & Herberstein, M. E. (2011). High-performance spider webs: integrating biomechanics, ecology and behaviour. *Journal of the Royal Society Interface, 8*(57), 457-471. doi: DOI 10.1098/rsif.2010.0454

Hayashi, C. Y., Blackledge, T. A., & Lewis, R. V. (2004). Molecular and mechanical characterization of aciniform silk: uniformity of iterated sequence modules in a novel member of the spider silk fibroin gene family. *Mol Biol Evol, 21*(10), 1950-1959. doi: 10.1093/molbev/msh204

Hayashi, C. Y., & Lewis, R. V. (2000). Molecular architecture and evolution of a modular spider silk protein gene. *Science, 287*(5457), 1477-1479.

Heim, M., Keerl, D., & Scheibel, T. (2009). Spider Silk: From Soluble Protein to Extraordinary Fiber. *Angewandte Chemie-International Edition, 48*(20), 3584-3596. doi: DOI 10.1002/anie.200803341

Heim, M., Romer, L., & Scheibel, T. (2010a). Hierarchical structures made of proteins. The complex architecture of spider webs and their constituent silk proteins. *Chemical Society Reviews, 39*(1), 156-164. doi: Doi 10.1039/B813273a

Heim, M., Romer, L., & Scheibel, T. (2010b). Hierarchical structures made of proteins. The complex architecture of spider webs and their constituent silk proteins. *Chem Soc Rev, 39*(1), 156-164. doi: 10.1039/b813273a

Humphrey, W., Dalke, A., & Schulten, K. (1996). VMD: Visual molecular dynamics. *Journal of Molecular Graphics, 14*(33).

Keten, S., & Buehler, M. J. (2010). Atomistic model of the spider silk nanostructure. *Applied Physics Letters, 96*(15), 153701. doi: 10.1063/1.3385388

Keten, S., & Buehler, M. J. (2010). Nanostructure and molecular mechanics of spider dragline silk protein assemblies. *J R Soc Interface, 7*(53), 1709-1721. doi: 10.1098/rsif.2010.0149

Keten, S., & Buehler, M. J. (2010). Nanostructure and molecular mechanics of spider dragline silk protein assemblies. *Journal of the Royal Society Interface*.

Keten, S., Xu, Z., Ihle, B., & Buehler, M. J. (2010). Nanoconfinement controls stiffness, strength and mechanical toughness of beta sheet crystals in silk. *Nature Materials, 9*(4), 359-367. doi: 10.1038/nmat2704

10.1038/NMAT2704

Kohler, T., & Vollrath, F. (1995). Thread Biomechanics in the 2 Orb-Weaving Spiders Araneus-Diadematus (Araneae, Araneidae) and Uloborus-Walckenaerius (Araneae, Uloboridae). *Journal of Experimental Zoology, 271*(1), 1-17.

Krink, T., & Vollrath, F. (1997). Analysing Spider Web-building Behaviour with Rule-based Simulations and Genetic Algorithms. *Journal of Theoretical Biology, 185*(3), 321-331. doi: http://dx.doi.org/10.1006/jtbi.1996.0306

Lin, L. H., Edmonds, D. T., & Vollrath, F. (1995). Structural-Engineering of an Orb-Spiders Web. *Nature, 373*(6510), 146-148.

Lin, L. H., & Sobek, W. (1998). Structural hierarchy in spider webs and spiderweb-type system. *The Structural Engineer, 76*(4), 59-64.

Madsen, B., Shao, Z. Z., & Vollrath, F. (1999). Variability in the mechanical properties of spider silks on three levels: interspecific, intraspecific and intraindividual. *Int J Biol Macromol, 24*(2-3), 301-306.

Nova, A., Keten, S., Pugno, N. M., Redaelli, A., & Buehler, M. J. (2010). Molecular and Nanostructural Mechanisms of Deformation, Strength and Toughness of Spider Silk Fibrils. *Nano Letters, 10*(7), 2626-2634.

Omenetto, F. G., & Kaplan, D. L. (2010). New opportunities for an ancient material. *Science, 329*(5991), 528-531. doi: 10.1126/science.1188936

Opell, B. D. (1994). Factors Governing the Stickiness of Cribellar Prey Capture Threads in the Spider Family Uloboridae. *Journal of Morphology, 221*(1), 111-119.

Opell, B. D. (1996). Functional similarities of spider webs with diverse architectures. *American Naturalist, 148*(4), 630-648.

Opell, B. D. (1997). A comparison of capture thread and architectural features of deinopoid and araneoid orb-webs. *Journal of Arachnology, 25*(3), 295-306.

Opell, B. D. (1998). Economics of spider orb-webs: the benefits of producing adhesive capture thread and of recycling silk. *Functional Ecology, 12*(4), 613-624.

Opell, B. D. (1999). Redesigning spider webs: Stickiness, capture area and the evolution of modern orb-webs. *Evolutionary Ecology Research, 1*(4), 503-516.

Opell, B. D., & Bond, J. E. (2001). Changes in the mechanical properties of capture threads and the evolution of modern orb-weaving spiders. *Evolutionary Ecology Research, 3*(5), 567-581.

Penney, D., & Ortuno, V. M. (2006). Oldest true orb-weaving spider (Araneae : Araneidae). *Biology Letters, 2*(3), 447-450. doi: DOI 10.1098/rsbl.2006.0506

Perea, G. B., Plaza, G. R., Guinea, G. V., Elices, M., Velasco, B., & Perez-Rigueiro, J. (2013). The variability and interdependence of spider viscid line tensile properties. *J Exp Biol, 216*(Pt 24), 4722-4728. doi: 10.1242/jeb.094011

Perez-Rigueiro, J., Plaza, G. R., Torres, F. G., Hijar, A., Hayashi, C., Perea, G. B., . . . Guinea, G. V. (2010). Supercontraction of dragline silk spun by lynx spiders (Oxyopidae). *Int J Biol Macromol, 46*(5), 555-557. doi: 10.1016/j.ijbiomac.2010.03.013

Peters, H. M. (1995). Ultrastructure of Orb Spiders Gluey Capture Threads. *Naturwissenschaften, 82*(8), 380-382.

Plimpton, S. J. (1995). Fast parallel algorithms for short-range molecular dynamics. *Journal of Computational Physics, 117*, 1-19.

Rammensee, S., Slotta, U., Scheibel, T., & Bausch, A. R. (2008). Assembly mechanism of recombinant spider silk proteins. *Proceedings of the National Academy of Sciences, 105*(18), 6590-6595. doi: 10.1073/pnas.0709246105

Rising, A., Widhe, M., Johansson, J., & Hedhammar, M. (2010). Spider silk proteins: recent advances in recombinant production, structure–function relationships and biomedical applications. *Cellular and Molecular Life Sciences, 68*(2), 169-184. doi: 10.1007/s00018-010-0462-z

Romer, L., & Scheibel, T. (2008). The elaborate structure of spider silk Structure and function of a natural high performance fiber. *Prion, 2*(4), 154-161.

S.W. Cranford , A. T., N. Pugno, M.J. Buehler. (2011). Nonlinear material behaviour of spider silk yields robust webs. *Nature*.

Selden, P. A. (1989). Orb-Web Weaving Spiders in the Early Cretaceous. *Nature, 340*(6236), 711-713.

Sen, D., & Buehler, M. J. (2011). Structural hierarchies define toughness and defect-tolerance despite simple and mechanically inferior brittle building blocks. *Scientific Reports, 1*(1), 35.

Sensenig, A., Agnarsson, I., & Blackledge, T. A. (2010). Behavioural and biomaterial coevolution in spider orb webs. *Journal of Evolutionary Biology, 23*(9), 1839-1856. doi: DOI 10.1111/j.1420-9101.2010.02048.x

Sensenig, A. T., Lorentz, K. A., Kelly, S. P., & Blackledge, T. A. (2012). Spider orb webs rely on radial threads to absorb prey kinetic energy. *Journal of the Royal Society Interface*. doi: rsif.2011.0851 [pii]

10.1098/rsif.2011.0851

Sherman, P. M. (1994). The Orb-Web - an Energetic and Behavioral Estimator of a Spiders Dynamic Foraging and Reproductive Strategies. *Animal Behaviour, 48*(1), 19-34.

Spivak, D., Giesa, T., Wood, L., & Buehler, M. J. (2011). Category Theoretic Analysis of Hierarchical Protein Materials and Social Networks. *PLoS ONE, 6*(http://dx.plos.org/10.1371/journal.pone.0023911).

Swanson, B. O., Anderson, S. P., Digiovine, C., Ross, R. N., & Dorsey, J. P. (2009). The evolution of complex biomaterial performance: The case of spider silk. *Integr Comp Biol, 49*(1), 21-31. doi: 10.1093/icb/icp013

Swanson, B. O., Blackledge, T. A., Beltrán, J., & Hayashi, C. Y. (2005). Variation in the material properties of spider dragline silk across species. *Applied Physics A, 82*(2), 213-218. doi: 10.1007/s00339-005-3427-6

Swanson, B. O., Blackledge, T. A., & Hayashi, C. Y. (2007). Spider capture silk: performance implications of variation in an exceptional biomaterial. *Journal of Experimental Zoology Part A: Ecological Genetics and Physiology, 307A*(11), 654-666. doi: 10.1002/jez.420

Tarakanova, A., & Buehler, M. J. (2012). A Materiomics Approach to Spider Silk--Protein Molecules to Webs. *JOM, 64*(2), 214-225.

Tian, M., & Lewis, R. V. (2005). Molecular characterization and evolutionary study of spider tubuliform (eggcase) silk protein. *Biochemistry, 44*(22), 8006-8012. doi: 10.1021/bi050366u

Tillinghast, E. K., Townley, M. A., Wight, T. N., Uhlenbruck, G., & Janssen, E. (1993). The Adhesive Glycoprotein of the Orb Web of Argiope-Aurantia (Araneae, Araneidae). *Biomolecular Materials, 292*, 9-23.

Tso, I. M., Wu, H. C., & Hwang, I. R. (2005). Giant wood spider Nephila pilipes alters silk protein in response to prey variation. *J Exp Biol, 208*(Pt 6), 1053-1061. doi: 10.1242/jeb.01437

van Beek, J. D., Hess, S., Vollrath, F., & Meier, B. H. (2002). The molecular structure of spider dragline silk: Folding and orientation of the protein backbone. *Proceedings of the National Academy of Sciences of the United States of America, 99*(16), 10266-10271.

Vepari, C., & Kaplan, D. L. (2007). Silk as a Biomaterial. *Prog Polym Sci, 32*(8-9), 991-1007. doi: 10.1016/j.progpolymsci.2007.05.013

Vollrath, F. (1999). Biology of spider silk. *International Journal of Biological Macromolecules, 24*, 81-88.

Vollrath, F. (2010). Spider Silk: Evolution and 400 Million Years of Spinning, Waiting, Snagging, and Mating. *Nature, 466*(7304), 319-319. doi: Doi 10.1038/466319a

Vollrath, F., Fairbrother, W. J., Williams, R. J. P., Tillinghast, E. K., Bernstein, D. T., Gallagher, K. S., & Townley, M. A. (1990). Compounds in the Droplets of the Orb Spiders Viscid Spiral. *Nature, 345*(6275), 526-528.

Vollrath, F., Madsen, B., & Shao, Z. (2001). The effect of spinning conditions on the mechanics of a spider's dragline silk. *Proc Biol Sci, 268*(1483), 2339-2346. doi: 10.1098/rspb.2001.1590

Vollrath, F., & Mohren, W. (1985). Spiral geometry in the garden spider's orb web *Naturwissenschaften, 72*(12), 666-667.

Vollrath, F., & Selden, P. (2007). The Role of Behavior in the Evolution of Spiders, Silks, and Webs. *Annual Review of Ecology, Evolution, and Systematics, 38*(1), 819-846. doi: 10.1146/annurev.ecolsys.37.091305.110221

Vollrath, F., & Tillinghast, E. K. (1991). Glycoprotein Glue beneath a Spider Webs Aqueous Coat. *Naturwissenschaften, 78*(12), 557-559.

Xu, M., & Lewis, R. V. (1990). Structure of a protein superfiber: spider dragline silk. *Proc Natl Acad Sci U S A, 87*(18), 7120-7124.

Zschokke, S. (2003). Spider-web silk from the Early Cretaceous. *Nature, 424*(6949), 636-637. doi: Doi 10.1038/424636a

Zschokke, S., & Vollrath, F. (1995). Web Construction Patterns in a Range of Orb-Weaving Spiders (Araneae). *European Journal of Entomology, 92*(3), 523-541.